

## **Copyright Warning & Restrictions**

The copyright law of the United States (Title 17, United States Code) governs the making of photocopies or other reproductions of copyrighted material.

Under certain conditions specified in the law, libraries and archives are authorized to furnish a photocopy or other reproduction. One of these specified conditions is that the photocopy or reproduction is not to be “used for any purpose other than private study, scholarship, or research.” If a user makes a request for, or later uses, a photocopy or reproduction for purposes in excess of “fair use” that user may be liable for copyright infringement,

This institution reserves the right to refuse to accept a copying order if, in its judgment, fulfillment of the order would involve violation of copyright law.

**Please Note: The author retains the copyright while the New Jersey Institute of Technology reserves the right to distribute this thesis or dissertation**

Printing note: If you do not wish to print this page, then select “Pages from: first page # to: last page #” on the print dialog screen

The Van Houten library has removed some of the personal information and all signatures from the approval page and biographical sketches of theses and dissertations in order to protect the identity of NJIT graduates and faculty.

## ABSTRACT

### EQUIVALENT CIRCUIT ANALYSIS OF A SEVENTH ORDER BANDPASS LOUDSPEAKER SYSTEM

by  
**Michael Gunnar Johnson**

A seventh order bandpass loudspeaker system was designed using an equivalent circuit analysis. The electrical, mechanical and acoustic systems were each modeled as separate subcircuits derived by using a Voltage-Force-Pressure or impedance analogy; the interactions between the subcircuits were modeled using coupled controlled-sources. The equivalent circuit was analyzed using SPICE (Simulation Program with Integrated Circuit Emphasis). A technique for modeling port and cavity resonances inside the enclosure using distributed element approximations for the resonant components was developed and verified by measurement.

A complete microcomputer based experimental loudspeaker testing system was designed incorporating a sweep frequency oscillator, a gain-controlled audio power amplifier, a true rms microphone interface, and a 12-bit, multiplexed, 100 ksamples/second A/D data acquisition system connected to an IBM compatible personal computer.

The frequency response of the system, as measured by a microphone in dB SPL (decibels, Sound Pressure Level), agreed with the predicted response to within 2 dB in the passband. Above the bandpass cutoff frequency, peaks in the response are shown to be caused by port and enclosure cavity resonances; dips in the response are shown by finite element modal analysis to be caused by enclosure wall resonances.

The technique of modeling the electro-mechanical-acoustic system using an equivalent circuit analysis with distributed element resonant components has been shown to be a valid design tool for high-order loudspeaker systems.

Blank Page

**EQUIVALENT CIRCUIT ANALYSIS OF A SEVENTH  
ORDER BANDPASS LOUDSPEAKER SYSTEM**

by  
**Michael Gunnar Johnson**

**A Thesis  
Submitted to the Faculty of  
New Jersey Institute of Technology  
in Partial Fulfillment of the Requirements for the Degree of  
Master of Science in Mechanical Engineering**

**Department of Mechanical Engineering**

**May 1997**

Copyright © 1997 by Michael Gunnar Johnson  
ALL RIGHTS RESERVED

APPROVAL PAGE

EQUIVALENT CIRCUIT ANALYSIS OF A SEVENTH  
ORDER BANDPASS LOUDSPEAKER SYSTEM

Michael Gunnar Johnson

---

Dr. Ira Cochín, Thesis Advisor Date  
Professor of Mechanical Engineering, NJIT

---

Dr. Rong-Yaw Chen, Committee Member Date  
Professor of Mechanical Engineering, NJIT

---

Dr. Zhiming Ji, Committee Member Date  
Associate Professor of Mechanical Engineering, NJIT

## BIOGRAPHICAL SKETCH

**Author:** Michael Gunnar Johnson

**Degree:** Master of Science

**Date:** May, 1997

### **Undergraduate and Graduate Education:**

- Master of Science in Mechanical Engineering  
New Jersey Institute of Technology, Newark, NJ, 1997
- Bachelor of Science in Mechanical Engineering  
New Jersey Institute of Technology, Newark, NJ, 1996
- Associate in Engineering, Mechanical Engineering Technology  
Pennsylvania State University, University Park, PA, 1983

**Major:** Mechanical Engineering

### **Presentations and Publications:**

- W. C. Bowman, J. R. Bailey, C. W. Boettcher, M. G. Johnson, F. M. Magalhaes, W. A. Nitz, F. Sarasola, G. R. Westerman, N. G. Ziesse, "A High Density Board Mounted Power Module for Distributed Power Systems," *Proceedings of the Fifth Annual IEEE Applied Power Electronics Conference and Exposition*, Los Angeles, CA, March 11-16, 1990.
- R. C. Frye, C. L. Hui, M. G. Johnson, "Noise and Routing Considerations in the Design of Mixed-Signal Silicon-on-Silicon Multichip Modules," *Proceedings of the 1994 ISHM Symposium and Exhibition on Microelectronics*, Boston MA, November 15-17, 1994.
- W. D. Simmons, M. G. Johnson, B. J. Han, R. C. Frye, "A Silicon-on-Silicon MCM Base-Band Controller for a Spread Spectrum Radio," *Proceedings of the Fifth International Conference and Exhibition on Multichip Modules*, Denver CO, April 17-19, 1996.



To my beloved wife Gina, for her patience over the years;  
and to my father, and the memory of my mother.

## ACKNOWLEDGMENT

I would like to express my sincere appreciation to Dr. Ira Cochlin, who not only served as my thesis advisor, but also provided insight and encouragement. Special thanks are given to Dr. Rong-Yaw Chen, and Dr. Zhiming Ji for actively participating in my committee.

I would also like to thank my friends and colleagues at Lucent Technologies for their assistance: Frederick T. Dickens, retired, and Dr. Robert M. Honeycutt: my mentors at Bell Laboratories, who nurtured my interest in acoustics; Daniel A. Quinlan for allowing me to borrow the laboratory grade test microphone; George Knoedl Jr., Anthony Bisconti, and Josef Ocenasek, for their help with the circuit design of the test set when I was stymied.

This work was performed under the Local University Part-Time Program at Lucent Technologies.

## TABLE OF CONTENTS

Chapter	Page
1 INTRODUCTION .....	1
1.1 Objective .....	1
1.2 Background Information .....	1
2 EQUIVALENT CIRCUIT MODEL .....	7
2.1 Impedance Analogy .....	7
2.2 Coupled Controlled-Source Transformations .....	10
2.3 Dual Voice Coil Driver Model .....	11
2.4 Lumped Parameter Equivalent Circuit .....	14
2.5 Frequency Response of the Lumped Parameter Model .....	17
2.6 Distributed Element Approximations for the Resonant Components .....	19
2.7 Complete Seventh Order Bandpass Equivalent Circuit .....	20
2.8 Predicted Frequency Response with Port and Cavity Resonances .....	22
3 MEASUREMENTS .....	26
3.1 Frequency Response Test Set Description .....	26
3.2 Measured Results .....	29
4 FINITE ELEMENT ANALYSIS .....	33
4.1 Enclosure Resonances .....	33
4.2 Comparison with Measured Results .....	34
5 CONCLUSIONS .....	37
APPENDIX A MEASUREMENT OF DRIVER PARAMETERS .....	38
APPENDIX B LUMPED PARAMETER EQUIVALENT CIRCUIT NETLIST ..	42
APPENDIX C MATHCAD CALCULATIONS FOR THE ENCLOSURE .....	43
APPENDIX D COMPLETE EQUIVALENT CIRCUIT NETLIST .....	51

**TABLE OF CONTENTS**  
**(Continued)**

<b>Chapter</b>	<b>Page</b>
APPENDIX E MECHANICAL DRAWING OF THE ENCLOSURE .....	54
APPENDIX F TEST SET DATA ACQUISITION PROGRAM LISTING .....	55
APPENDIX G FIRST THIRTY VIBRATION MODES OF THE ENCLOSURE .	60
REFERENCES .....	75

## LIST OF TABLES

Table	Page
2.1 Voltage-Force-Pressure or Impedance Analogy: Symbols and SI Units .....	9
4.1 First Thirty Resonant Frequencies of the Enclosure .....	35

## LIST OF FIGURES

Figure	Page
2.1 Driver Cross Section; Equivalent Mechanical, Electrical Representations .....	7
2.2 Controlled-Source Interactions, Impedance Analogy .....	10
2.3 Electromechanical Equivalent Circuit of a Dual Voice Coil Driver .....	12
2.4 Lumped Parameter Model of the Seventh Order Bandpass System .....	15
2.5 Frequency Response of the Lumped Parameter Model .....	18
2.6 Lumped and Distributed Element Approximations - Resonant Components ....	19
2.7 Complete Seventh Order Bandpass Equivalent Circuit .....	21
2.8 Frequency Response of the System Including Resonances .....	23
2.9 Electrical Impedance of the System in Ohms .....	24
2.10 Cone Displacement ( $m_v = mm$ , rms) .....	25
2.11 Velocity of Air in the Ports ( $A = m/s$ , rms) .....	25
3.1 Block Diagram of the Frequency Response Test Set .....	27
3.2 Test Set Frequency Calibration Curve .....	28
3.3 Predicted and Measured System Frequency Response .....	30
3.4 Frequency Response of the System with Damping Material .....	31
4.1 Finite Element Mesh for the Enclosure Analysis .....	33
4.2 Mode Shape Example from Appendix G: $f = 236.27$ Hz .....	36
4.3 System Frequency Response without Averaging .....	36
E.1 Mechanical Drawing of the Enclosure .....	54
G.1 Enclosure Mode Shape 1: $f = 236.27$ Hz .....	60
G.2 Enclosure Mode Shape 2: $f = 259.17$ Hz .....	60
G.3 Enclosure Mode Shape 3: $f = 446.13$ Hz .....	61
G.4 Enclosure Mode Shape 4: $f = 459.73$ Hz .....	61
G.5 Enclosure Mode Shape 5: $f = 470.82$ Hz .....	62

**LIST OF FIGURES**  
**(Continued)**

<b>Figure</b>	<b>Page</b>
G.6 Enclosure Mode Shape 6: $f = 488.78$ Hz .....	62
G.7 Enclosure Mode Shape 7: $f = 504.25$ Hz .....	63
G.8 Enclosure Mode Shape 8: $f = 517.50$ Hz .....	63
G.9 Enclosure Mode Shape 9: $f = 520.27$ Hz .....	64
G.10 Enclosure Mode Shape 10: $f = 575.61$ Hz .....	64
G.11 Enclosure Mode Shape 11: $f = 592.40$ Hz .....	65
G.12 Enclosure Mode Shape 12: $f = 663.46$ Hz .....	65
G.13 Enclosure Mode Shape 13: $f = 730.33$ Hz .....	66
G.14 Enclosure Mode Shape 14: $f = 766.32$ Hz .....	66
G.15 Enclosure Mode Shape 15: $f = 853.73$ Hz .....	67
G.16 Enclosure Mode Shape 16: $f = 870.25$ Hz .....	67
G.17 Enclosure Mode Shape 17: $f = 897.04$ Hz .....	68
G.18 Enclosure Mode Shape 18: $f = 927.51$ Hz .....	68
G.19 Enclosure Mode Shape 19: $f = 941.49$ Hz .....	69
G.20 Enclosure Mode Shape 20: $f = 1018.9$ Hz .....	69
G.21 Enclosure Mode Shape 21: $f = 1030.0$ Hz .....	70
G.22 Enclosure Mode Shape 22: $f = 1037.9$ Hz .....	70
G.23 Enclosure Mode Shape 23: $f = 1046.4$ Hz .....	71
G.24 Enclosure Mode Shape 24: $f = 1096.4$ Hz .....	71
G.25 Enclosure Mode Shape 25: $f = 1122.2$ Hz .....	72
G.26 Enclosure Mode Shape 26: $f = 1131.5$ Hz .....	72
G.27 Enclosure Mode Shape 27: $f = 1223.4$ Hz .....	73
G.28 Enclosure Mode Shape 28: $f = 1247.6$ Hz .....	73
G.29 Enclosure Mode Shape 29: $f = 1290.2$ Hz .....	74

**LIST OF FIGURES**  
**(Continued)**

<b>Figure</b>	<b>Page</b>
G.30 Enclosure Mode Shape 30: $f = 1292.1$ Hz .....	74



# CHAPTER 1

## INTRODUCTION

### 1.1 Objective

The objective of this thesis is to present the application of the method of equivalent circuit analysis to the design of high order loudspeaker systems using multiple voice coil drivers. If equivalent circuit analysis is applicable, then reasonable agreement between predicted and measured results should be obtained, and the technique will be shown to be a valid design tool for these systems.

### 1.2 Background Information

The need for the solution of the problems connected with long distance telephone signal transmission has led to many important advancements in electrical network and filter theory. One of the unexpected outcomes of the early research in this field at what was then Bell Telephone Laboratories was the application of the principles of electrical network theory to the design of vibrating mechanical systems. Maxfield and Harrison [1] in their paper "Methods of High Quality Recording and Reproducing of Music and Speech Based on Telephone Research," published in 1926, documented the early history of this technique. As early as 1912, electrical network theory principles were applied to the mechanical design of telephone receivers [2],[3].

Although the moving-coil loudspeaker was patented in 1898 [4], the widespread application of electrical analog circuits to loudspeaker system design did

not occur until 1954, when B.B. Bauer published a paper [5] in which he describes the use of transformers as circuit elements to model the electrical-to-mechanical and mechanical-to-acoustic interactions. The transformer coupling technique was also derived by Beranek in his *Acoustics* [6], a classic text on the subject published in 1954.

In the transformer coupling method of analysis, all electrical component impedances are first transformed to the mechanical equivalent circuit by the turns ratio of the electrical-to-mechanical transformer; then all mechanical component impedances are transformed to the acoustical circuit by the turns ratio of the mechanical-to-acoustic transformer. The result is one circuit which contains the acoustic elements along with the transformed mechanical elements and the twice transformed electrical elements. With one circuit describing the entire system, the transfer function could be obtained. This method of modeling was used in the landmark papers of Thiele [7], and Small [8],[9],[10], in the analysis of closed-box and vented bass-reflex loudspeaker systems. Their analysis formed the foundation of low-frequency loudspeaker system design: the minimum number of driver constants which are required for the design of a loudspeaker system are now known as the Thiele-Small parameters, which are published on data sheets for all drivers available today from reputable manufacturers.

A problem arises when the transformer technique is applied to the design of loudspeaker systems. Using the Voltage-Force-Pressure or Impedance Analogy, a force across an element is treated as a voltage in the mechanical equivalent circuit; but this force (a *voltage*) is derived from the *current* in the electrical circuit (force equals the cross product of the current-length and magnetic B field vectors). The current-to-

voltage transformation requires an impedance inversion, the results of which can be confusing. For example, a crossover network inductor which is connected electrically in series with the voice coil becomes a capacitor connected in parallel in the acoustic equivalent circuit. The results are very counter-intuitive.

In 1991, Leach [11] described the application of the popular electrical circuit simulation program SPICE (Simulation Program with Integrated Circuit Emphasis) to the analysis of electroacoustic systems. SPICE is a circuit simulation program that was developed in the 1970's to assist in the electrical design of integrated circuits, and today is one of the most widely used among electrical engineers. Leach applied the use of coupled controlled-source components which are normally used in SPICE to model active devices like transistors (a simple model of a transistor is a current-controlled current source - a small current into the base terminal controls a proportionally larger current in the collector) to the electrical-to-mechanical and mechanical-to-acoustic transformations in the equivalent circuit. The use of controlled-sources to model the electrical to mechanical transformation eliminates the awkward impedance inversion required by the transformer technique. Leach derives the equivalent circuit for both closed box and vented loudspeaker systems.

When coupled controlled-sources are used to model the electrical-to-mechanical and the mechanical-to-acoustic interactions, each part of the equivalent circuit is modeled separately: the electrical, mechanical and the acoustic circuits are each separate circuits, but they are coupled through the interactions of the controlled-sources. The need for combining the separate subsystems into one circuit is eliminated.

The units for the elements in each subcircuit are now clear: electrical units are used in the electrical circuit, mechanical units are used in the mechanical circuit and acoustical units are used in the acoustical circuit. Further, series elements appear in series and parallel elements appear in parallel in each subcircuit.

In recent years there has been an increasing market demand for high performance, compact loudspeaker systems. However, the design guidelines for simple closed box [9] and vented bass reflex systems [7], [10] clearly show the dependence of system frequency response and efficiency on enclosure size. Traditionally, efficient low frequency loudspeaker systems were large, because to move enough air to create audible sounds at low frequencies, large drivers were required; the larger the driver, the larger the enclosure must be to get flat frequency response.

In 1989, Geddes published “An Introduction to Band-Pass Loudspeaker Systems” [12] in which he derives by use of the transformer coupling technique the transfer functions for fourth through eighth order bandpass systems. Bandpass loudspeaker enclosures are generally cabinets which completely surround the driver, and have at least two internal compartments, one or more of which may be vented. These systems employ coupled resonance to increase the driver efficiency over a small range of frequencies, resulting in extended low frequency performance and more compact enclosure size than can be obtained from simple closed box or vented bass reflex enclosures.

Geddes used a “nondescript” driver in his bandpass simulations, the parameters of which he “manipulated to achieve whatever characteristics were required,”

presumably to achieve a flat frequency response. He used an unnamed “algebra processor” to derive the analytic equations for the transfer functions that appear in the appendix of his paper which are based on a lumped parameter analysis and therefore do not model the port resonance which he concludes is the most important factor in selecting the order of the system in an application. In the body of his paper, he used an unnamed “numerical simulator” to model the systems, and all frequency response curves show the effects of port resonance on the output: exactly how the port resonance was modeled is not explained. No measured results are shown.

Geddes shows that the seventh order bandpass system is a good choice for bandpass systems, because it results in high efficiency and wide bandwidth while also providing adequate attenuation of port resonance. Geddes states that the transfer function for the passive eighth order system was not derived because undesirable electrical impedance characteristics resulted. For these reasons, the seventh order system was chosen for this design.

Three questions are left to be answered. 1) Can a seventh order bandpass system be designed using a commercially available driver, or is a custom driver design necessary? 2) Can the equivalent circuit analysis technique be extended to model port resonances, and if so, how? 3) How is a driver with multiple voice coils modeled?

In this thesis, Leach's controlled-source technique is extended to the design of a seventh order bandpass loudspeaker system that will be used for a subwoofer. The equivalent circuit for a commercially available dual voice coil driver is derived, and a technique is described for modeling the cavity and port resonances in the enclosure

using distributed element approximations. Finally, predicted results are compared with measurements on a working system.

## CHAPTER 2

### EQUIVALENT CIRCUIT MODEL

#### 2.1 Impedance Analogy

In Figure 2.1, a simplified cross-section drawing of a moving-coil loudspeaker driver is shown (a) along with its equivalent mechanical representation (b) and an electrical equivalent circuit (c). In Figure 2.1(a), the moving mass of the system is comprised of the voice coil, the coil former, the cone, and the dustcap. The cone is connected to the frame by the compliant suspension. Further, it can be seen that the magnet structure, polarized North and South as shown, is arranged so that the magnetic  $B$  field is everywhere perpendicular to the voice coil windings. When a current  $i$  flows in the voice coil of total wire length  $l$ , a force  $f$  will act on the moving mass. The force generated by the voice coil is determined by the vector equation shown: force equals the cross product of the *current\*length* and the magnetic  $B$  field vectors, here the force is simply the current  $i$  multiplied by the  $Bl$  product.

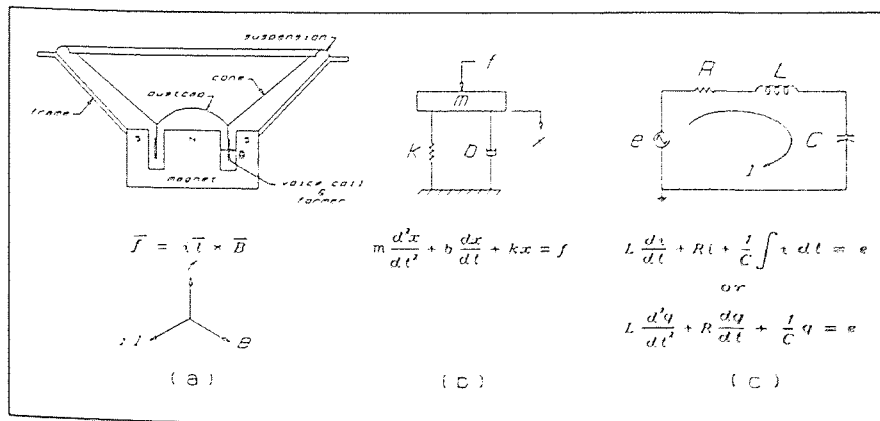


Figure 2.1 Driver Cross Section; Equivalent Mechanical, Electrical Representations

The mechanical representation is shown in Figure 2.1(b). Here  $m$  represents the moving mass of the system,  $k$  represents the effective mechanical spring constant of the suspension, and  $b$  represents the effective damping coefficient of the suspension. The element labeled  $f$  is the driving force for the system. The mechanical system equation is determined by applying d'Alembert's principle to a free body diagram of the moving mass  $m$ , and is shown in the figure.

The electrical diagram shown in Figure 2.1(c) is a series  $R$ - $L$ - $C$  circuit connected to a voltage generator  $e$ . The symbols  $i$  and  $q$  represent current and electrical charge respectively. The electrical system equation is determined by applying Kirchoff's Voltage Law to the circuit and is shown in the figure in two forms, one in terms of current, and the other in terms of electrical charge.

Note that the electrical system equation written in terms of electrical charge  $q$  is similar to the mechanical system equation. When the differential equations describing two systems are similar, the systems are said to be analogous, and the solution of one system can be applied to the other and vice versa. In this pair of systems, the analogous quantities are: Force  $f$  and Voltage  $e$ , Mass  $m$  and Inductance  $L$ , Damping Coefficient  $b$  and Resistance  $R$ , Reciprocal Spring Constant or Compliance  $1/k$  and Capacitance  $C$ , Displacement  $x$  and Charge  $q$ , and Velocity  $\dot{x}$  and Current  $i$ . The representation of the two systems as shown is called the Force - Voltage analogy, or in Acoustics as the *Impedance* analogy.

Note that in the impedance analogy, the components in the electrical equivalent circuit are connected in series. Another representation exists in which the electrical



components are connected in parallel. The parallel representation is known in Acoustics as the *Mobility* analogy, which will not be discussed here. The interested reader can refer to Beranek [6], Chapter 3, and Cochlin [13], Section 3.6. In this thesis, only the Impedance analogy is used.

So far, only the equivalent circuit for the mechanical system has been discussed. Next, the analogous components for the acoustical system will be developed. The components in the acoustical equivalent circuit are similar to those in the mechanical system. Again, using the Impedance analogy, Acoustic Mass  $M_A$  is analogous to Inductance  $L$ , Acoustic Compliance  $C_A$  is analogous to Capacitance  $C$ , Acoustic Resistance  $R_A$  is analogous to Resistance  $R$  and Acoustic Pressure  $p$  is analogous to Voltage  $e$ . Table 2.1 summarizes the components and symbols used in the Impedance analogy and the SI units used in each system.

**Table 2.1** Voltage - Force - Pressure or Impedance Analogy: Symbols and SI Units

Electrical System	Mechanical System	Acoustic System
Voltage $e$ (Volts)	Force $f$ (N)	Pressure $p$ (Pa)
Current $i$ (Amperes)	Velocity $u$ (m/s)	Volume Flow Rate $U$ (m <sup>3</sup> /s)
Charge $q$ (Coulombs)	Displacement $x$ (m)	Volume Displacement $V$ (m <sup>3</sup> )
Inductance $L$ (Henries)	Mass $m$ (kg)	Acoustic Mass $M_A$ (kg/m <sup>4</sup> )
Capacitance $C$ (Farads)	Compliance $1/k$ (m/N)	Acoustic Compliance $C_A$ (m <sup>5</sup> /N)
Resistance $R$ (Ohms)	Damping Coefficient $b$ (N*s/m)	Acoustic Resistance $R_A$ (N*s/m <sup>5</sup> )

## 2.2 Coupled Controlled-Source Transformations

Following Leach [11], the coupled controlled-source transformations using the impedance analogy for the electrical-to-mechanical and mechanical-to-acoustic circuits are shown in Figure 2.2. In Figure 2.2(a), two current-controlled voltage sources are used to model the electrical-to-mechanical transformation. The force generator in the mechanical circuit is a voltage source whose magnitude is controlled by the current in the electrical circuit. Similarly, to model the mechanical back EMF in the electrical circuit, a voltage source which is controlled by the current in the mechanical circuit (which represents velocity) is used. In both cases the proportionality constant is set equal to the  $Bl$  product parameter of the driver.

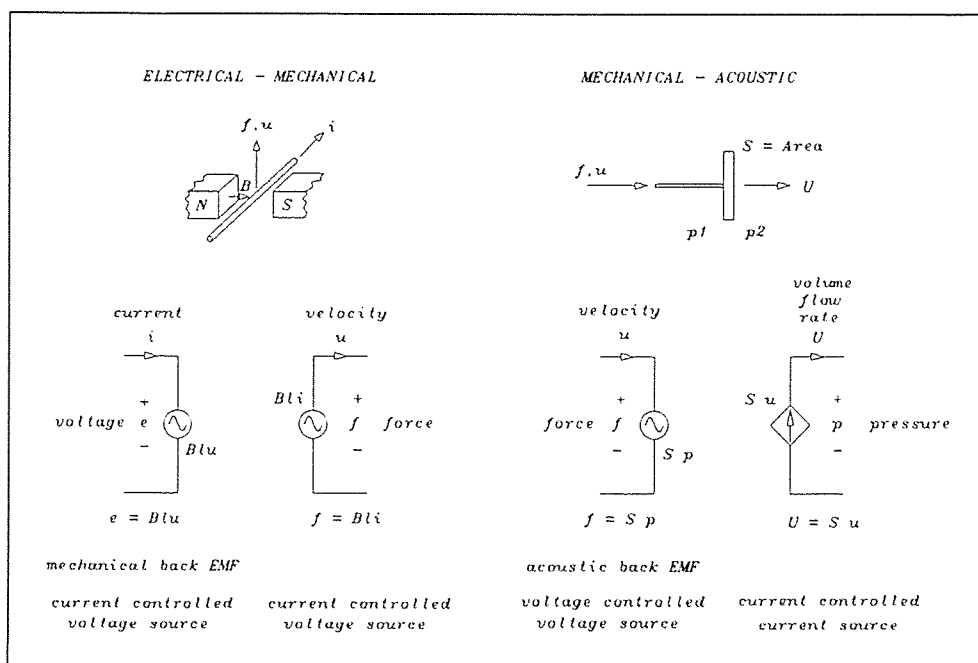


Figure 2.2 Controlled-Source Interactions, Impedance Analogy

The mechanical-to-acoustic interaction is shown in Figure 2.2(b). Here, a current-controlled current source is used to convert the velocity (mechanical current) of the driver cone to an acoustic volume flow rate of air (acoustic current). Similarly, a voltage-controlled voltage source in the mechanical circuit models the acoustic back EMF: a pressure (acoustic voltage) wave impinging on the driver cone results in a net force (mechanical voltage). The proportionality constant for these sources is the effective cross-sectional area of the driver cone.

### 2.3 Dual Voice Coil Driver Model

Recently loudspeaker driver manufacturers have introduced low frequency drive units which incorporate two identical voice coils mounted on the same coil-former and cone assembly. These drivers allow greater flexibility in the design of enclosures, since the designer has the option of a) using both voice coils connected together in series, b) using both coils connected together in parallel, c) using only one voice coil and using the other for velocity feedback, or d) using both voice coils, driving each from a separate stereo channel. The last option may appear contradictory, since it converts a stereo system to a “monophonic” one. However, there is little stereo separation at very low frequencies due to the long wavelengths of the signals. More importantly, the enclosure volume for a dual voice coil driver is half the size of what would be required if two drivers were mounted in the same enclosure and driven from both channels of a stereo system. The term “subwoofer” has been commonly used to describe stereo

loudspeaker arrangements which use a single enclosure intended to be used only for the lowest frequencies in a system.

The electromechanical equivalent circuit for a dual voice coil driver with both coils driven separately is shown in Figure 2.3. The first electrical system is composed of an electrical generator labeled  $eg1$ , a resistor  $Re1$  and an inductor  $Le1$  which model the DC resistance and the inductance of the voice coil winding, a current-controlled voltage source labeled  $HBLU1$ , and a “dummy” voltage source  $VD1$ . In SPICE, the current-controlled current source and the current-controlled voltage sources both require the name of a constant voltage source through which the controlling current flows. The voltage source  $VD1$  is really an ammeter: to measure a current in SPICE an AC voltage source is used whose value is set to zero. The second electrical system is identical to the first, except for different label numbers.

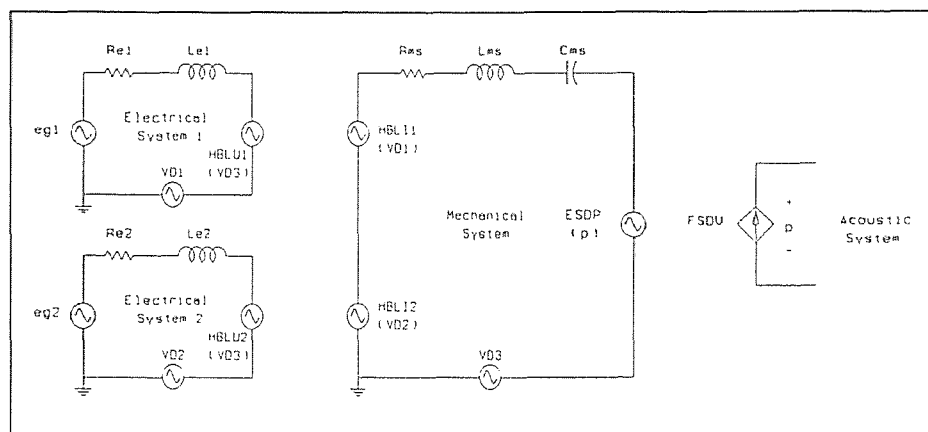


**Figure 2.3** Electromechanical Equivalent Circuit of a Dual Voice Coil Driver

The mechanical system consists of the components  $R_{ms}$  - the mechanical system damping resistance,  $L_{ms}$  - the mechanical system mass,  $C_{ms}$  - the mechanical system compliance, two current controlled voltage sources labeled HBLI1 and HBLI2, a voltage-controlled voltage source labeled ESDP, and another “dummy” voltage source ammeter labeled VD3.

The acoustic generator labeled FSDU is shown with voltage nodes on either side labeled  $p^+$  and  $p^-$ . The acoustic system components connect to this source.

The electrical-to-mechanical interaction for the first voice coil is modeled by the coupled current-controlled voltage sources HBLU1 and HBLI1. Note the name convention used: component names beginning with H are current-controlled voltage sources in SPICE. The next two letters indicate the constant of proportionality, here in each case it is the  $Bl$  product parameter. The next letter in the name indicates which current is controlling the source: on the mechanical side, the electrical current  $I_1$  (measured by VD1) controls the source, and on the electrical side, the mechanical current  $u$  (velocity, measured by VD3) is controlling the back EMF source. The second electrical-to-mechanical interaction is similar to the first, again except for the names. Note that the same current  $i(\text{VD3})$  controls both back EMF generators.

In the impedance analogy for the mechanical circuit, force is analogous to voltage. Here, with two voice coils being driven independently, there will be *two* force generators acting on the moving mass of the mechanical system. At low frequencies, the driving signals will be nearly identical. These forces must add to produce twice the force that would be present if only one coil were acting alone. The two voltage

sources modeling the force generators must be connected in series in the electrical equivalent circuit so that the voltages in the mechanical system (really the forces) add.

## 2.4 Lumped Parameter Equivalent Circuit

The seventh order bandpass system consists of a driver mounted in an enclosure with two ported chambers on either side, along with an inductor connected in series with the voice coil [12]. The seven important energy storage elements in the system are 1) the mechanical mass, 2) the suspension compliance of the driver, 3) the acoustic mass of air in the front chamber port, 4) the acoustic compliance of the air inside the front chamber volume, 5) the acoustic mass of air in the rear chamber port, 6) the acoustic compliance of the air in the rear chamber volume and, 7) the inductor in series with the voice coil.

The optimization of the parameters for flat frequency response in the seventh order system requires many iterations. The design proceeds quickly however if one begins by using a simplified “lumped parameter” model since there are only five components to vary: the front and rear enclosure volume capacitances, the front and rear port inductances, and the inductor in series with each voice coil. Once a reasonably flat frequency response is obtained, a more complicated model that will be discussed later can then be used to predict the final response more accurately.

A simplified controlled-source analogous circuit for a seventh order bandpass system using a dual-voice coil driver is shown in Figure 2.4. SPICE allows only one input source during a simulation, so the following technique was devised to drive both coils simultaneously: the subcircuit consisting of the components VEG and R1 is an

AC voltage source for the system; the components labeled EEG1 and EEG2 are voltage-controlled voltage sources that are controlled by the voltage at node 1, and the multiplication factor is set to unity. The result is two electrical generators which track the single input source VEG as it is swept in frequency.

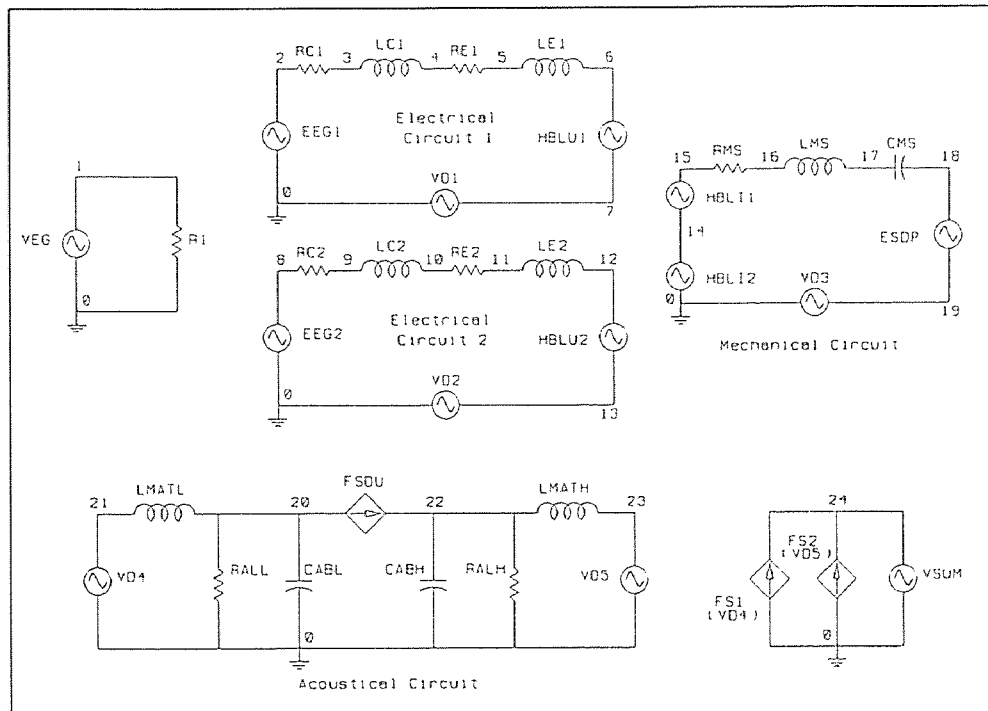


**Figure 2.4** Lumped Parameter Model of the Seventh Order Bandpass System

The components labeled RC1 and LC1 represent the DC resistance and inductance of the inductor that is connected in series with the first voice coil; RC2 and LC2 are the similar components for the inductor connected in series with the second voice coil. The other components in the electrical and mechanical circuits were discussed in section 2.3.

The acoustical system shown in Figure 2.4 is a simplified representation of an enclosure that uses two ported enclosures on either side of the driver. The component labeled CABH is the front chamber air volume compliance, RALH is a resistor which models air leaks in the front chamber, LMATH is an inductor which represents the acoustic mass of the air in the port of the front chamber. VD5 is an ammeter which measures the current through the inductor LMATH, and represents the volume flow rate of air in the port of the front chamber. Similarly, CABL, RALL, LMATL, and VD4 are the corresponding components for the rear chamber.

The components labeled FS1, FS2 and VSUM form a circuit which adds the volume flow rates of air in both ports. FS1 is a current-controlled current source with a multiplication factor set to unity and is controlled by the current in VD4. Similarly FS2 is controlled by the current through VD5. VSUM is an ammeter which measures the sum of the two currents.

The magnitude of the low frequency farfield on-axis acoustic rms pressure of the system at a distance  $r$  is [6]:

$$|p(r)| = \rho_o f |U_{sum}| / r$$

Where  $\rho_o$  is the density of air which is equal to  $1.18 \text{ kg/m}^3$ , and  $f$  is frequency in Hz.

The sound pressure level that would be measured by a microphone is [6]:

$$\text{SPL} = 20 \log_{10} [p(r) / p_{ref}]$$

where  $p_{ref}$  is equal to  $2 \cdot 10^{-5} \text{ N/m}^2$  or Pa. Combining these two equations results in the

SPICE postprocessor PROBE expression for sound pressure level:

At a microphone distance of 1 meter:



$$\text{SPL} = 20 * \log_{10} [59000 * \text{frequency} * i(\text{VSUM})]$$

At a distance of twelve inches:

$$\text{SPL}_{12} = 20 * \log_{10} [193570 * \text{frequency} * i(\text{VSUM})]$$

These expressions were programmed using the macro feature of PROBE. The one meter sound pressure level expression becomes SPL(VSUM), and the twelve inch expression is SPL12(VSUM).

Note that in this system, if the front and rear enclosure volumes and port air masses are set equal to one another, the output of each port will cancel the other since the air masses will be vibrating with equal amplitudes 180 degrees out of phase. To get useful output, the front and rear chambers must be tuned to different frequencies, one higher than and the other lower than the driver resonant frequency. The H and L suffixes in the acoustic component labels indicate which components are describing the high or low frequency enclosure compartments.

The measured values for the driver parameters are included in Appendix A. The SPICE netlist for the schematic diagram shown in Figure 2.4 is included in Appendix B.

## 2.5 Frequency Response of the Lumped Parameter Model

After many iterations, the frequency response shown in Figure 2.5 was obtained.

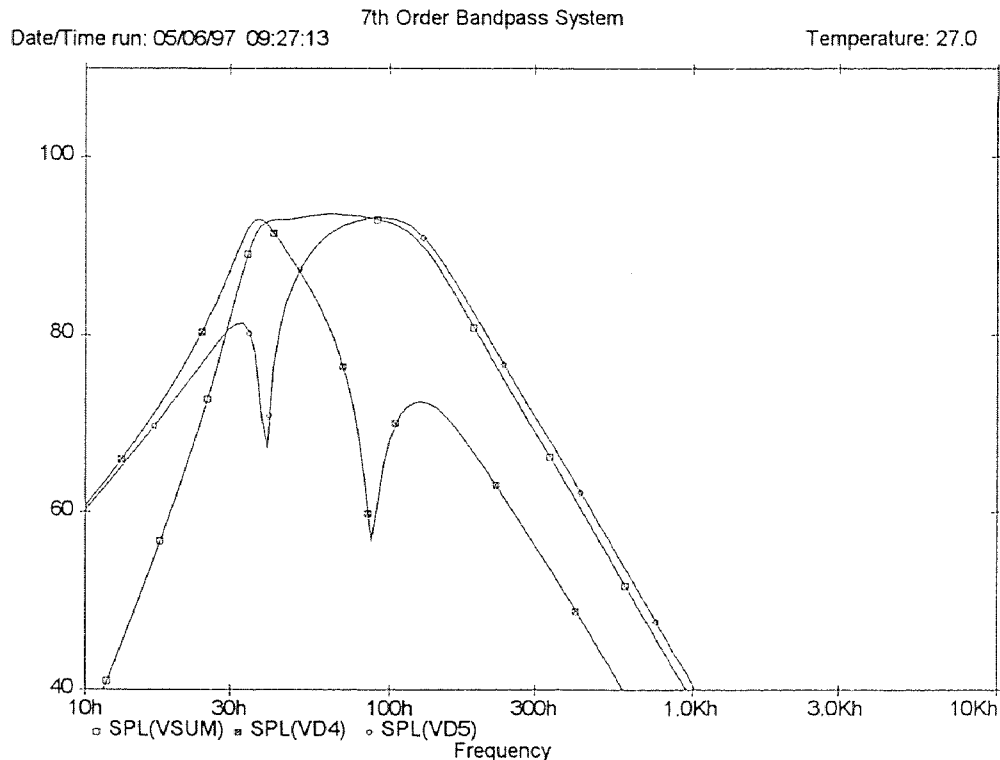


**Figure 2.5** Frequency Response of the Lumped Parameter Model

The final parameter component values can be found by referring to the SPICE netlist in Appendix B. Three curves are plotted in Figure 2.5: the first, SPL(VSUM) is the 1 meter on-axis sound pressure level output obtained by summing the volume flow rates of air in both ports. The curve SPL(VD4) is the response due to the low frequency port alone, and SPL(VD5) is the response due to the high frequency port. This response was obtained by varying the enclosure and series inductor parameters only. The measured driver parameters were never altered. The component values obtained from the lumped parameter netlist were then used to calculate the dimensions of the enclosure. The Mathcad calculations are included in Appendix C.

## 2.6 Distributed Element Approximations for the Resonant Components

The frequency response curve shown in Figure 2.5 shows a smooth continuous decrease above the high frequency cutoff point of the bandpass filter. In the body of his paper, Geddes [12] was able to somehow include the effects of the “pipe-organ” resonance of the ports in his simulations. How this was done is not described.

After many attempts at simulating the port resonance and comparing the results with measurements of working systems, it was found that the enclosure cavity resonance also needs to be considered when designing high order systems. The following method was developed to approximate the port and cavity resonances in the enclosure.

Figure 2.6 shows two alternate representations of the acoustic air mass of a port and the acoustic compliance of a volume of air inside an enclosure. The first representation shows the equations used to calculate the lumped parameter component values given the dimensions of the device.

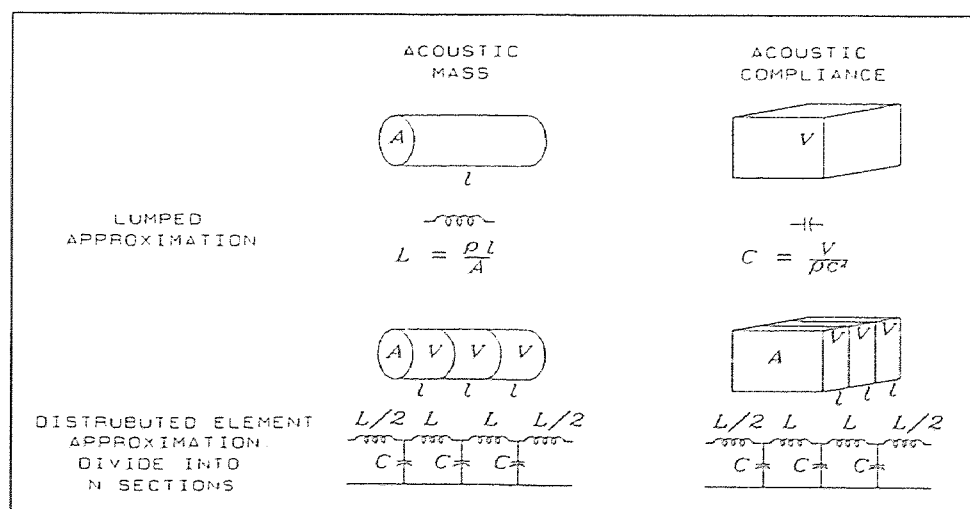


Figure 2.6 Lumped and Distributed Element Approximations - Resonant Components

The second representation shows the technique used to model the resonant version of each device. The port is divided into three imaginary sections, and an acoustic mass and acoustic compliance is calculated using the dimensions of the section. Node points are assigned at the central location of each section. The section compliance components are placed at these node points to ground (fixed reference). The section mass components are arranged as shown in the schematic - from each end to the first node point the distance is  $l/2$ , so  $1/2 L$  is used for the acoustic mass at the boundaries; between central nodes the distance is  $l$ , and the acoustic mass is therefore equal to  $L$  calculated from the section dimensions. The same method is used to develop the distributed element approximation for the enclosure compliances. Calculations for these components are included in Appendix C.

## 2.7 Complete Seventh Order Bandpass Equivalent Circuit

The final equivalent circuit for the system includes several components that can only be known once the enclosure has been defined. In addition to the distributed element approximation components for the ports and enclosure volumes, these include the effects of acoustic mass loading of the driver due to having a wall in close proximity (Leach [11]), and the acoustic radiation impedances of the ports (Beranek [6]). Again, calculations for all components are included in Appendix C.

The complete seventh order bandpass equivalent circuit is shown in Figure 2.7. The port and cavity resonance components are labeled. LMABH and LMABL are the components that model the mass loading of the enclosure on the driver. LMECL and LMECH are the inner end correction air masses from Beranek [6].

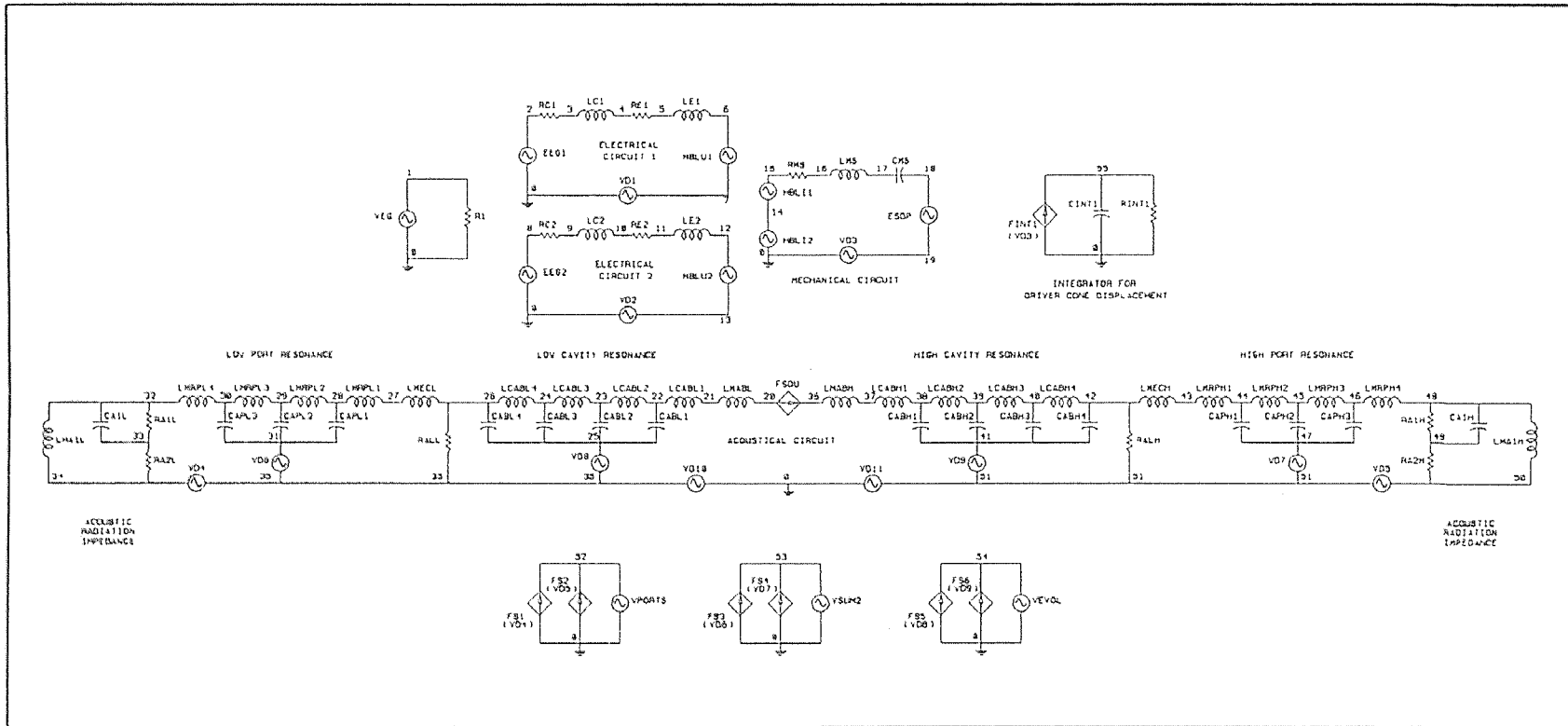


Figure 2.7 Complete Seventh Order Bandpass Equivalent Circuit

The components labeled VD8 and VD9 are voltage source ammeters which measure the volume flow rate of the air inside the enclosure. VD4 and VD5 measure the volume flow rates of the air in the ports. These are added, as before, using the source VPORTS. VEVOL is the sum of the enclosure volume flow rates.

An additional circuit was added to integrate the velocity in the mechanical circuit in order to measure the cone displacement. FINT1 is a current-controlled current source that is controlled by the current in VD3 - the current in the mechanical circuit which represents the mechanical velocity. The multiplication factor for FINT1 is set to unity, so that the current in amperes will correspond to velocity in meters per second. This current is integrated by the capacitor CINT1 whose value is set to 1 Farad. The voltage across a capacitor is equal to  $1/C$  multiplied by the integral of current with respect to time. With C set to a value of 1 Farad, the voltage across the capacitor in volts will be numerically equal to the cone displacement in meters.

## **2.8 Predicted Frequency Response with Port and Cavity Resonances**

Figure 2.8 shows the predicted on-axis 1 Watt, 1 meter frequency response of the system. The electrical source was set to 2.0 V, the rms AC voltage level for 1 Watt into 4 Ohms. All voltages and currents in the simulation will then be rms values. Comparing this result with Figure 2.5 shows a very different result above the bandpass cutoff frequency.

The lowest resonance is due not to a port resonance, but the low frequency cavity resonance. This effect was not modeled in the numerical simulation of Geddes

[12]. Notice also that there is a slight difference in the predicted results between the sound pressure level as calculated by the ports alone SPL(PORTS), and the one calculated using the enclosure volume flow rates SPL(VEVOL).

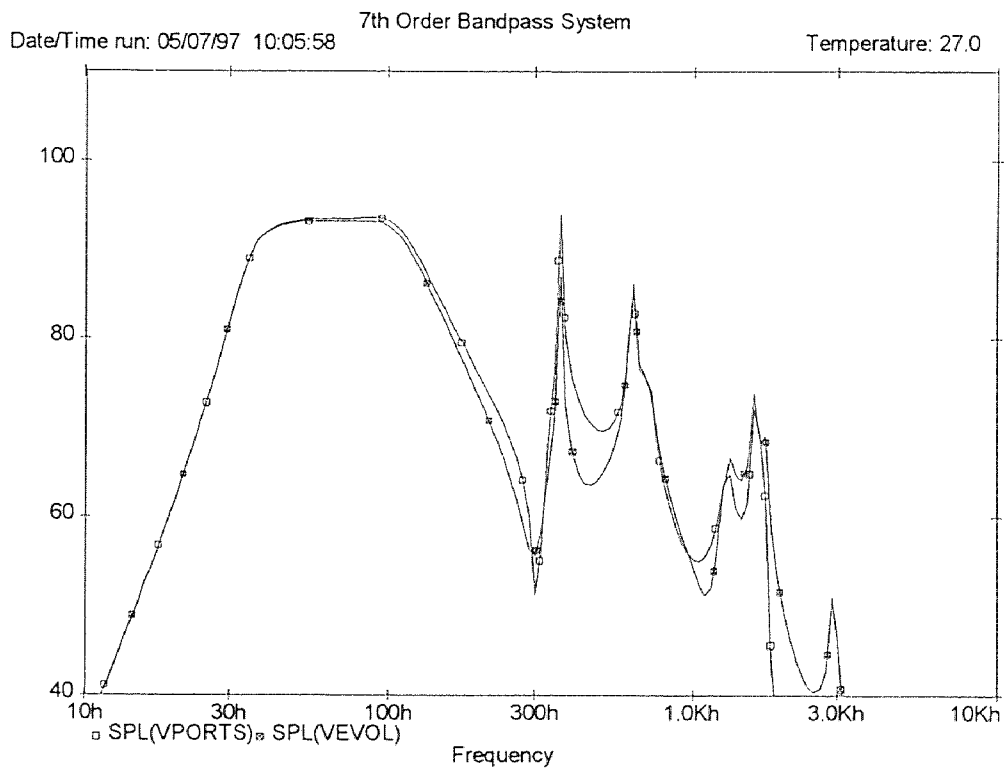


**Figure 2.8** Frequency Response of the System Including Resonances

The electrical impedance that the system presents to the amplifier is shown in Figure 2.9. This is simply the node voltage at the electrical source EEG2 divided by the current through the source. The peaks in the electrical impedance curve are the resonant frequencies in the system. The low and high frequency peaks are the resonant frequencies at which the high and low frequency enclosures are tuned. The middle peak is due to the mechanical resonant frequency of the driver.

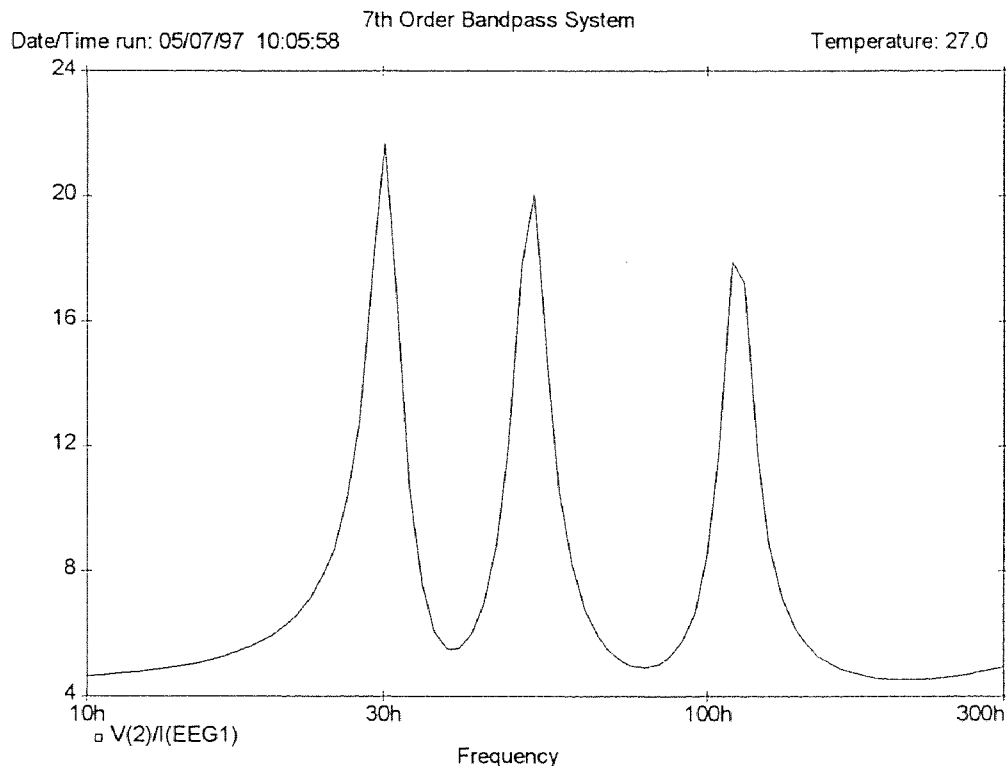


**Figure 2.9** Electrical Impedance of the System in Ohms

Figure 2.10 is the rms cone displacement as a function of frequency. Again, displacement is determined by plotting the integrator node voltage. The displacement in meters is numerically equal to the integrator node voltage in Volts. The largest displacement is approximately 2.3 mm, rms.

Figure 2.11 is a graph of rms air velocity in the ports. Air velocity is found by dividing the volume flow rates of air in the ports by the port area in square meters. For this graph, port area ( $S_p = 9 \text{ in}^2 = 5.8064 \times 10^{-3} \text{ m}^2$ ) was taken from the calculations in Appendix C. The highest air velocity occurs in the low frequency port and is equal to about 3 m/s, rms.



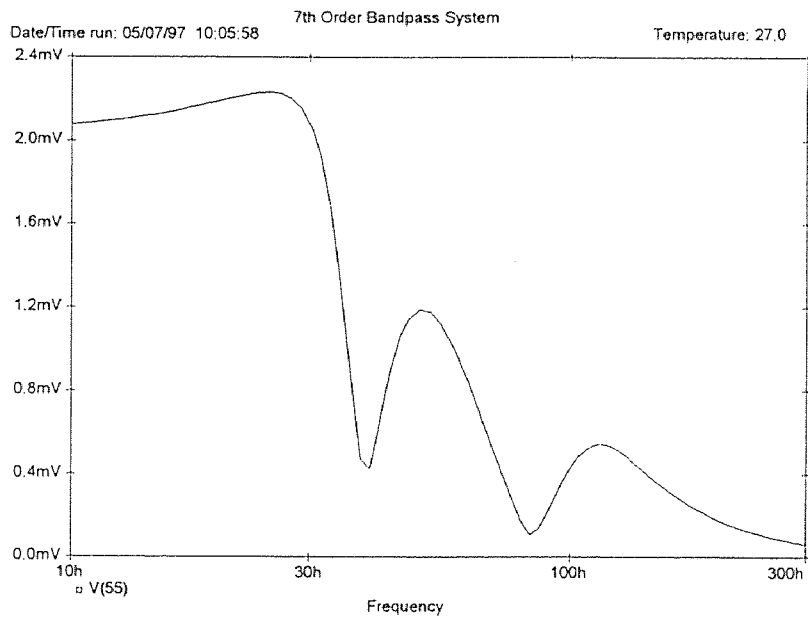


Figure 2.10 Cone Displacement (mV = mm, rms)

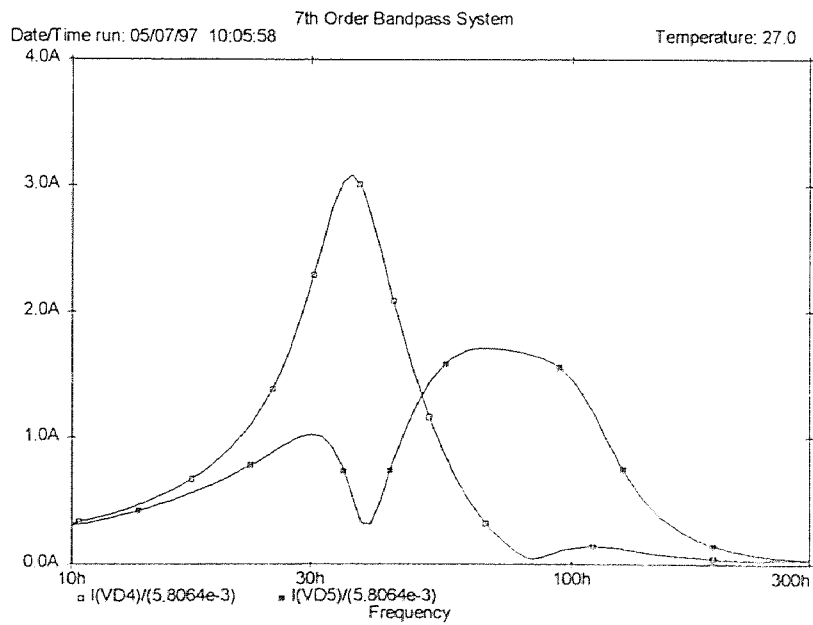


Figure 2.11 Velocity of Air in the Ports (A = m/s, rms)

## CHAPTER 3

### MEASUREMENTS

The system was constructed according to the dimensions calculated in Appendix C. The material used for the enclosure was 1/2" exterior grade plywood. The outside surfaces of the enclosure were covered with Formica laminate. A mechanical drawing of the enclosure is included in Appendix E.

#### 3.1 Frequency Response Test Set Description

Figure 3.1 shows a block diagram of the test set used to make the frequency response measurements. The system is built around a precision sinewave voltage controlled oscillator. The output of the oscillator is a constant voltage AC sinewave signal and a DC control voltage determines the output frequency. The log ramp circuit shown in Figure 3.1 applies a ramp voltage to the control pin of the oscillator that increases logarithmically as a function of time. The output of the oscillator is a constant voltage AC signal that sweeps in frequency logarithmically from 8 Hz to 21 kHz.

The output amplitude of the oscillator is modulated by an AGC (Automatic Gain Control) amplifier. The AGC circuit maintains a constant output signal amplitude at the loudspeaker terminals. The Audio Power Amplifier amplifies the signal and drives both voice coils simultaneously. A peak detector/level shifting circuit detects the peak voltage signal at the voice coil terminals and sends the appropriate control signal

to the AGC circuit to continuously compensate for any change in the amplitude of the signal at the voice coil terminals.

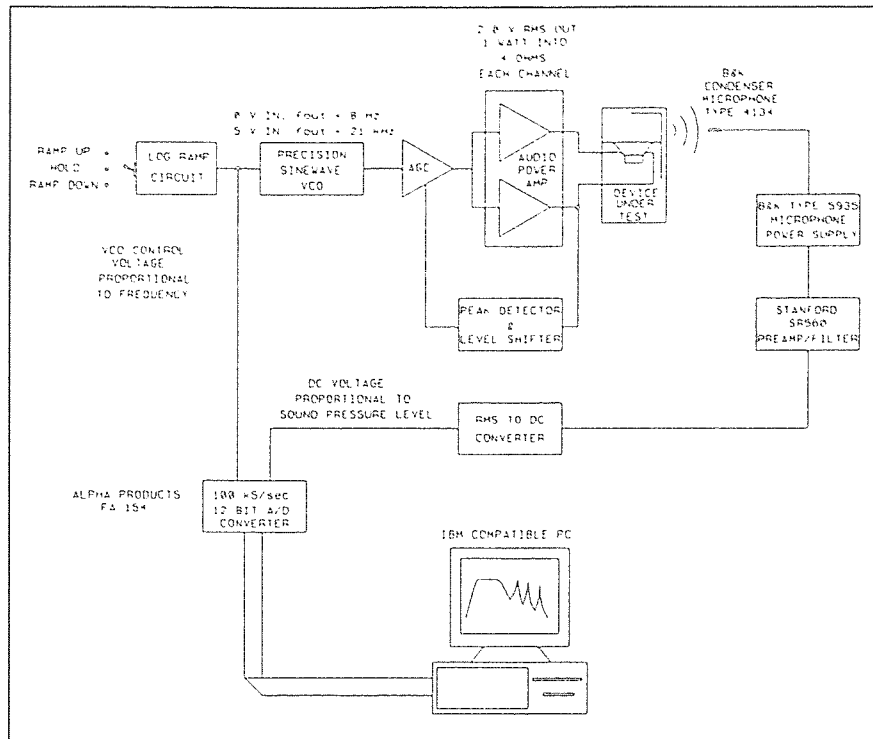


**Figure 3.1** Block Diagram of the Frequency Response Test Set

A laboratory grade test microphone was used to measure the sound pressure level output of the system. The microphone element used was a Bruel & Kjaer (B&K) Condenser Microphone Type 4134. The frequency response of this microphone element is flat to within  $\pm 2$  dB from 4 Hz to 20 kHz, calibration data was supplied. The microphone was powered by a B&K Type 5935 Microphone Power Supply, the gain of which was set to 20 dB, with output option set to linear. The Stanford Research Systems model SR560 Low Noise Preamplifier filter function was set to

bandpass, with cutoff frequencies of 3 Hz and 30 kHz, and its gain was set to unity.

The output of the preamplifier was connected to a true rms-to-DC converter circuit, whose DC output amplitude is proportional to the rms value of the AC output of the microphone preamplifier. This signal is proportional to the sound pressure level measured by the microphone.

The frequency of the system was measured by monitoring the slowly varying ramp voltage applied to the VCO. The frequency measurement was calibrated by measuring the frequency at fixed control voltage signals, and curve fitting the data to get an equation for output frequency as a function of input voltage. The frequency calibration curve is shown in Figure 3.2.

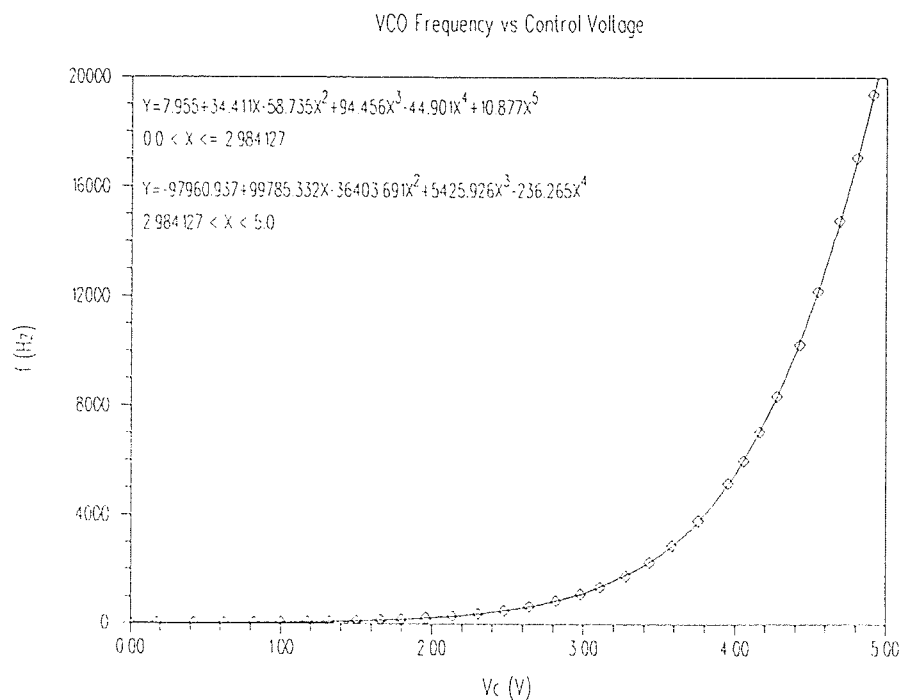


**Figure 3.2** Test Set Frequency Calibration Curve

The VCO control voltage signal and the rms-to-DC signal were monitored by an Alpha Systems model FA154 A/D (Analog-to-Digital) converter system connected to an IBM compatible personal computer. The data acquisition program was written in Microsoft QuickBASIC version 4.5 and the complete listing is included in Appendix F.

The sound pressure level measurement was calibrated using a B&K Sound Level Calibrator Type 4230. This device calibrates the microphone output level at a fixed frequency of 1 kHz with a constant amplitude sound pressure level of 94 dB SPL. The microphone system was connected to the test set, the calibrator was activated, then ten sound pressure level readings were averaged, and a SPL correction factor was calculated. The correction factor for the B&K microphone is included in the program listing of Appendix F.

### 3.2 Measured Results

The measurement of very low frequency loudspeaker systems is complicated by the long wavelengths of the signals. Standing waves are quickly established in even the largest rooms at a frequency of 30 Hz, which has a wavelength of approximately 36 feet.

Shearman [14] describes a technique of taking measurements outdoors to eliminate room boundaries. Small [15] described a technique in which the pressure *inside* the enclosure is measured (in any environment - even reverberant) from which the farfield response can be calculated. Keele [16] describes a similar technique of

measuring the nearfield sound pressure outside the enclosure from which the farfield response can be calculated.

In this measurement, a combination of outdoor measurements and nearfield techniques was used to evaluate the loudspeaker performance. The area in which the measurements were taken was not an open field, and two test sets were not available to measure both ports simultaneously at the very close range required by Keele's nearfield measurement technique. The measurements were made outdoors, on-axis at a distance of twelve inches to minimize the effect of reflections, while at the same time allowing the use of only one microphone to make the measurements.

Figure 3.3 shows the measured response of the system, measured outdoors, on-axis, at a distance of twelve inches. Superimposed on the same graph is the predicted response at twelve inches obtained from the SPICE model (See Section 2.4).

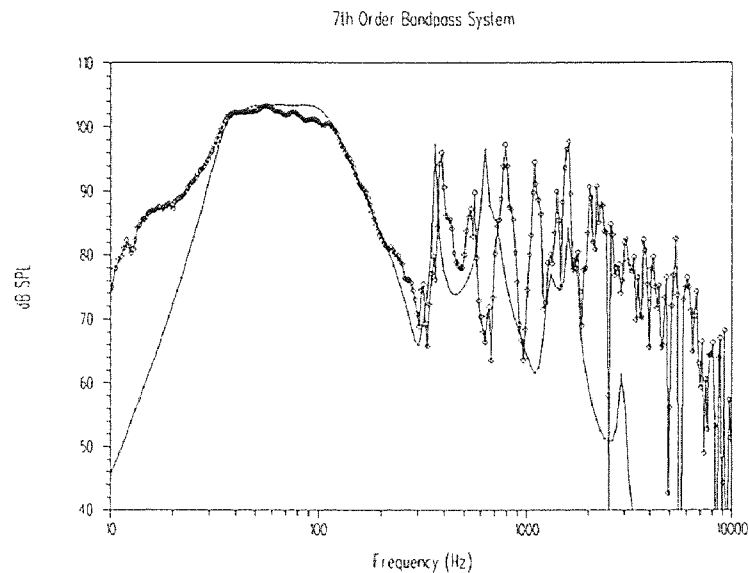


**Figure 3.3** Predicted and Measured System Frequency Response

The model predicts the actual behavior of the system quite accurately. The slight dip in frequency response in the bandpass region is probably due to the fact that the measurement conditions were not truly free of reflection boundaries. However, the bandpass cutoff frequencies are predicted quite well, as is the magnitude of the first resonance peak at approximately 370 Hz

The high peaks in the response curve due to resonance above the cutoff frequency are undesirable. In an attempt to control the intensity of these resonances, damping material was placed inside the enclosure cabinet. Very light polyester fiberfill material was placed inside both front and rear volumes of the enclosure. The damping material was placed inside both front and rear volumes of the enclosure. The damping material completely filled the volumes but was not compressed. No damping material was placed in the ports. The measured response with damping material is shown in Figure 3.4.

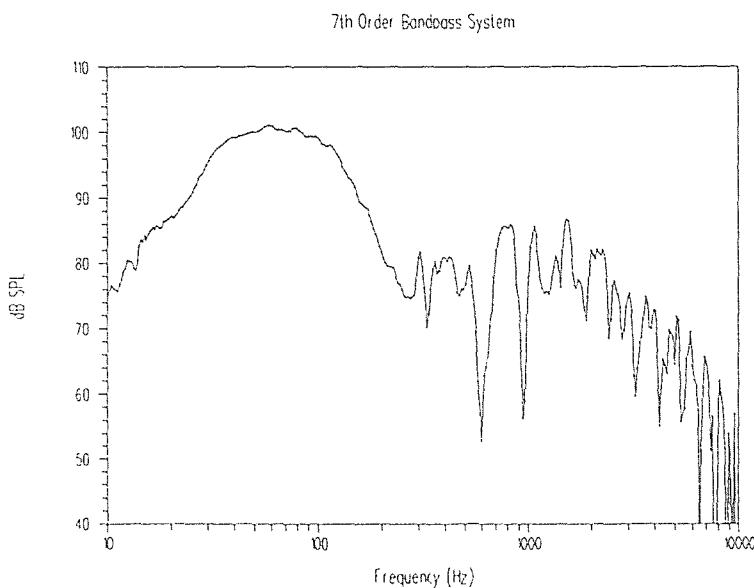


**Figure 3.4** Frequency Response of the System with Damping Material

The resonance problem is much improved and the bandpass response has not degraded significantly. The damping material inside the volume of the enclosure apparently controls the dominant resonance in this system: cavity resonance.



CHAPTER 4  
FINITE ELEMENT ANALYSIS

4.1 Enclosure Resonances

A finite element analysis was performed in order to determine the natural frequencies and mode shapes of the enclosure. The commercial FEA software program Algor was used in this analysis. Figure 4.1 shows the mesh that was used in the enclosure simulation.

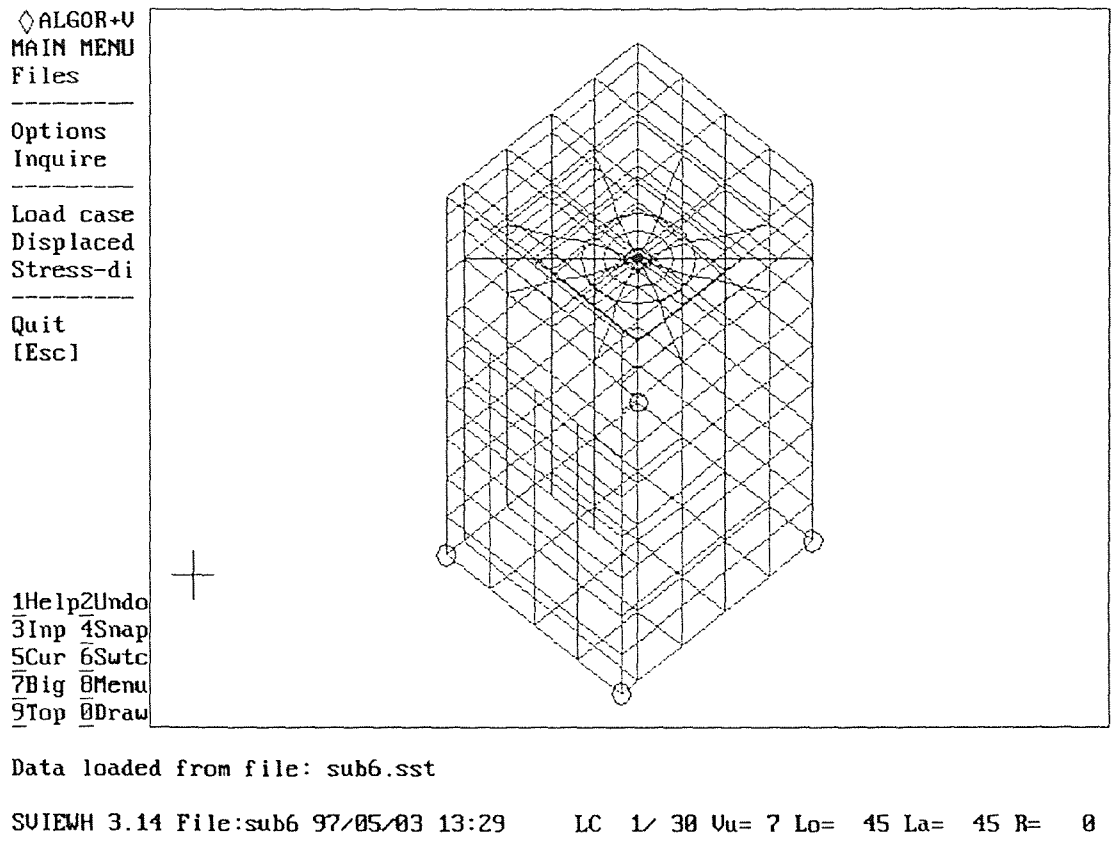


Figure 4.1 Finite Element Mesh for the Enclosure Analysis

The enclosure was modeled using 3-D plate/shell elements. The interior plates were 11.76 mm thick. The modulus of elasticity used was  $E = 10.9$  GPa. A small sample of the plywood used in the enclosure was weighed in order to estimate the density of  $0.64$  g/cm<sup>3</sup>. The exterior of the enclosure was covered with Formica, and plates used in the model for these surfaces were 13.06 mm thick. The density of the plywood sample covered with Formica was  $0.67$  g/cm<sup>3</sup>. The weight of the driver was modeled by changing the density of the elements in the center of the baffle plate inside the radius of the driver so that the total weight of these elements equaled 907.2 g, the measured weight of the driver. The enclosure was modeled as simply supported.

Table 4.1 is a portion of the output, listing the first 30 natural frequencies of the enclosure. Figure 4.2 shows the first mode shape for corresponding to  $f = 236.27$  Hz. The other mode shapes are included in Appendix G.

#### **4.2 Comparison with Frequency Response Results**

The measured frequency response plot shown in Figure 3.3 was averaged over every 15 points to reveal the structure. The data as taken without averaging, and no enclosure damping material is shown here in Figure 4.3. Note that groups of closely spaced “dips” in the frequency response are occurring at approximately 250-300 Hz, 400-500 Hz, 600-700 Hz, 900-1000 Hz and 1200 Hz. It appears as if these are caused by enclosure resonances. The enclosure resonances appear to be absorbing energy from the air inside the box that would have been used to drive the port air masses, causing drops in the output.

**Table 4.1** First Thirty Resonant Frequencies of the Enclosure.

mode number	circular frequency (rad/sec)	frequency (Hertz)	period (sec)	tolerance
1	1.4845E+03	2.3627E+02	4.2324E-03	2.1130E-16
2	1.6284E+03	2.5917E+02	3.8585E-03	7.0245E-16
3	2.8031E+03	4.4613E+02	2.2415E-03	2.3706E-16
4	2.8886E+03	4.5973E+02	2.1752E-03	0.0000E+00
5	2.9583E+03	4.7082E+02	2.1239E-03	2.1284E-16
6	3.0711E+03	4.8878E+02	2.0459E-03	3.9497E-16
7	3.1683E+03	5.0425E+02	1.9831E-03	7.4222E-16
8	3.2516E+03	5.1750E+02	1.9324E-03	1.7618E-16
9	3.2690E+03	5.2027E+02	1.9221E-03	5.2291E-16
10	3.6167E+03	5.7561E+02	1.7373E-03	2.8480E-16
11	3.7222E+03	5.9240E+02	1.6880E-03	5.3777E-16
12	4.1686E+03	6.6346E+02	1.5073E-03	4.2875E-16
13	4.5888E+03	7.3033E+02	1.3692E-03	2.1230E-15
14	4.8150E+03	7.6632E+02	1.3049E-03	3.2137E-16
15	5.3642E+03	8.5373E+02	1.1713E-03	1.2947E-16
16	5.4679E+03	8.7025E+02	1.1491E-03	3.3642E-15
17	5.6363E+03	8.9704E+02	1.1148E-03	4.6907E-16
18	5.8277E+03	9.2751E+02	1.0782E-03	5.6380E-14
19	5.9156E+03	9.4149E+02	1.0621E-03	6.3873E-16
20	6.4021E+03	1.0189E+03	9.8143E-04	5.1191E-12
21	6.4718E+03	1.0300E+03	9.7085E-04	5.9823E-13
22	6.5212E+03	1.0379E+03	9.6350E-04	4.9492E-11
23	6.5747E+03	1.0464E+03	9.5567E-04	4.6087E-11
24	6.8887E+03	1.0964E+03	9.1210E-04	3.0584E-10
25	7.0510E+03	1.1222E+03	8.9111E-04	2.0020E-08
26	7.1094E+03	1.1315E+03	8.8378E-04	4.6007E-09
27	7.6866E+03	1.2234E+03	8.1742E-04	3.3090E-08
28	7.8388E+03	1.2476E+03	8.0155E-04	6.1671E-06
29	8.1067E+03	1.2902E+03	7.7506E-04	7.6185E-06
30	8.1183E+03	1.2921E+03	7.7395E-04	7.0785E-08

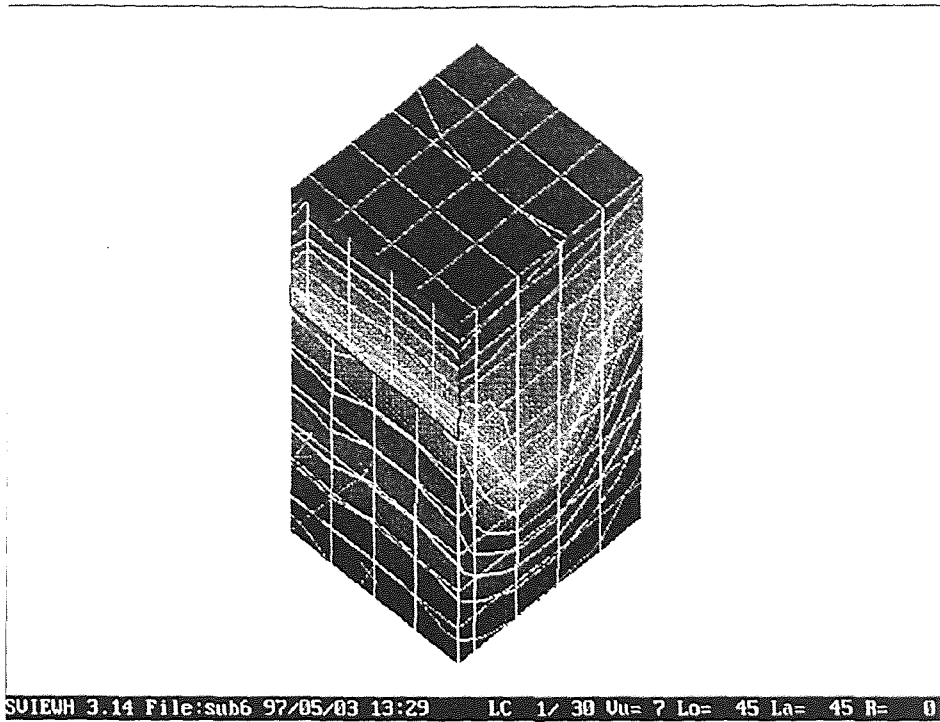


Figure 4.2 Mode Shape Example from Appendix G:  $f = 236.27$  Hz

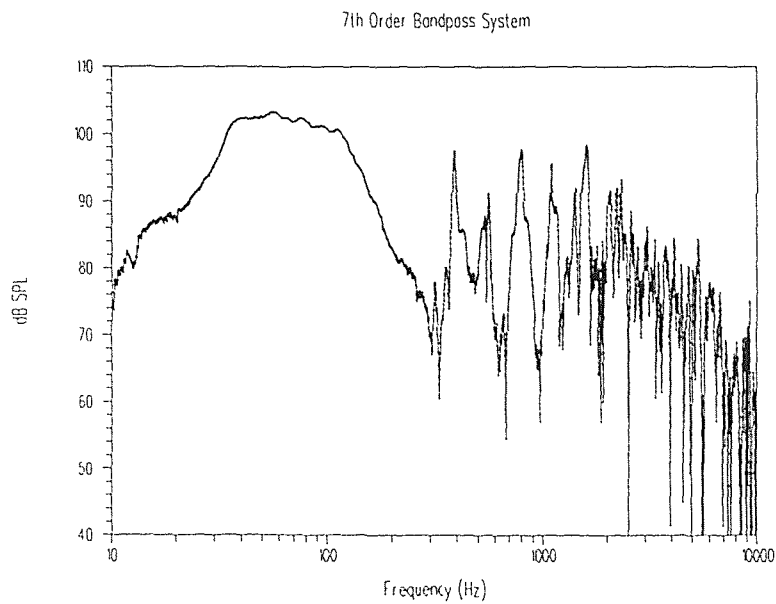


Figure 4.3 System Frequency Response without Averaging

## CHAPTER 5

### CONCLUSIONS

A seventh order bandpass loudspeaker system has been successfully constructed using a commercially available dual voice coil driver. An equivalent circuit for the dual voice coil driver was developed using two electrical circuits and one mechanical circuit in which has the force generators placed in series. The technique of modeling the enclosure cavity and port resonances using distributed element approximations for the resonant components was successfully verified by measurements on a working system. The method of equivalent circuit analysis has been shown to be an effective tool for handling complex problems in high-performance loudspeaker design.

Measured results show excellent agreement with the prediction, as long as the observer is careful to make the measurements using a calibrated microphone in a non-reverberant environment.

Enclosure wall resonances do not appear to adversely affect the acoustic output of the system, but port and more significantly, enclosure cavity resonances do. These were shown to be easily controlled by using damping material inside the volumes of the enclosure.

An improvement to this analysis technique would involve including the effects of enclosure damping material inside the enclosure in the equivalent circuit model. This is a subject for future work.

## APPENDIX A

### MEASUREMENT OF DRIVER PARAMETERS

Driver Parameters from Test Measurements

File: apxa1.mcd

Measurements:

Radio Shack # 40-1373 6.5" Dual Voice Coil Driver Voice Coil #1  
Constant Voltage Resistance Ratio Measurements Using Rknown = 5.2 Ohms

$$R_e := 3.6225 \text{ Ohms}$$

$$R_{max} := 19.9251 \text{ Ohms}$$

$$F_s := 56.1 \text{ Hz}$$

$$R_o := \frac{R_{max}}{R_e} \quad R_o = 5.5 \text{ Ohms}$$

$$R_x := \sqrt{R_o \cdot R_e} \quad R_x = 8.496 \text{ Ohms}$$

The corresponding frequencies at which  $Z = R_x$  are:

$$F_1 := 44.38 \text{ Hz}$$

$$F_2 := 69.78 \text{ Hz}$$

From the Added Mass Method: from Beranek [6], p.229.

$$M := \frac{25.25}{1000} \text{ kg}$$

$$F_{sp} := 34.19 \text{ Hz}$$

From Small [9]:

$$Q_{ms} := \frac{F_s \cdot \sqrt{R_o}}{(F_2 - F_1)} \quad Q_{ms} = 5.18$$

$$Q_{es} := \frac{Q_{ms}}{(R_o - 1)} \quad Q_{es} = 1.151$$

$$Q_{ts} := \frac{Q_{es} \cdot Q_{ms}}{(Q_{es} + Q_{ms})} \quad Q_{ts} = 0.942$$

And:

$$C_{ms} := \frac{1}{M \cdot (2 \cdot \pi)^2} \left[ \frac{(F_s + F_{sp}) \cdot (F_s - F_{sp})}{(F_s \cdot F_{sp})^2} \right] \quad C_{ms} = 5.394 \cdot 10^{-4} \text{ m/N}$$

Then

$$M_{ms} := \frac{1}{(2 \cdot \pi \cdot F_s)^2 \cdot C_{ms}} \quad M_{ms} = 0.015 \quad \text{kg}$$

$$R_{ms} := \frac{(2 \cdot \pi \cdot F_s) \cdot M_{ms}}{Q_{ms}} \quad R_{ms} = 1.015 \quad \text{N*s/m}$$

$$B_l := \sqrt{\frac{2 \cdot \pi \cdot F_s \cdot R_e \cdot M_{ms}}{Q_{es}}} \quad B_l = 4.068 \quad \text{T*m}$$

From Beranek [6]:

$$a := 0.0648 \quad \text{m} \quad \text{radius of driver}$$

$$\rho_0 := 1.18 \quad \text{kg/m}^3 \quad \text{density of air}$$

$$M_{m1} := 2.67 \cdot a^3 \cdot \rho_0 \quad \text{air load mass on the two sides of the diaphragm}$$

$$M_{m1} = 8.573 \cdot 10^{-4}$$

$$M_{md} := \frac{M}{\left(\frac{F_s}{F_{sp}}\right)^2 - 1} - M_{m1}$$

$$M_{md} = 0.014 \quad \text{kg}$$

Voice Coil Inductance Using Z @ 1500 Hz and 10000 Hz:

$$f_1 := 1500 \quad Z_1 := 6.2392 \quad \text{Ohms}$$

$$\omega_1 := 2 \cdot \pi \cdot f_1$$

$$f_2 := 10005 \quad Z_2 := 17.117 \quad \text{Ohms}$$

$$\omega_2 := 2 \cdot \pi \cdot f_2$$

$$L_e := \sqrt{\frac{Z_2^2 - Z_1^2}{\omega_2^2 - \omega_1^2}}$$

$$L_e = 2.565 \cdot 10^{-4} \quad \text{H}$$

Driver Parameters from Test Measurements

File:apxa2.mcd

Measurements:

Radio Shack # 40-1373 6.5" Dual Voice Coil Driver Voice Coil #2  
Constant Voltage Resistance Ratio Measurements Using Rknown = 5.2 Ohms

$$R_e := 3.5505 \quad \text{Ohms}$$

$$R_{\max} := 19.4496 \quad \text{Ohms}$$

$$F_s := 55.52 \quad \text{Hz}$$

$$R_o := \frac{R_{\max}}{R_e} \quad R_o = 5.478 \quad \text{Ohms}$$

$$R_x := \sqrt{R_o \cdot R_e} \quad R_x = 8.31 \quad \text{Ohms}$$

The corresponding frequencies at which  $Z = R_x$  are:

$$F_1 := 43.82 \quad \text{Hz}$$

$$F_2 := 70.41 \quad \text{Hz}$$

From the Added Mass Method: from Beranek [6], p.229.

$$M := \frac{25.25}{1000} \quad \text{kg}$$

$$F_{sp} := 34.33 \quad \text{Hz}$$

From Small [9]:

$$Q_{ms} := \frac{F_s \cdot \sqrt{R_o}}{(F_2 - F_1)} \quad Q_{ms} = 4.887$$

$$Q_{es} := \frac{Q_{ms}}{(R_o - 1)} \quad Q_{es} = 1.091$$

$$Q_{ts} := \frac{Q_{es} \cdot Q_{ms}}{(Q_{es} + Q_{ms})} \quad Q_{ts} = 0.892$$

And:

$$C_{ms} := \frac{1}{M \cdot (2 \cdot \pi)^2} \left[ \frac{(F_s + F_{sp}) \cdot (F_s - F_{sp})}{(F_s \cdot F_{sp})^2} \right] \quad C_{ms} = 5.258 \cdot 10^{-4} \quad \text{m/N}$$



Then

$$M_{ms} = \frac{1}{(2 \cdot \pi \cdot F_s)^2 \cdot C_{ms}} \quad M_{ms} = 0.016 \quad \text{kg}$$

$$R_{ms} = \frac{(2 \cdot \pi \cdot F_s) \cdot M_{ms}}{Q_{ms}} \quad R_{ms} = 1.116 \quad \text{N*s/m}$$

$$Bl = \sqrt{\frac{2 \cdot \pi \cdot F_s \cdot Re \cdot M_{ms}}{Q_{es}}} \quad Bl = 4.212 \quad \text{T*m}$$

From Beranek [6]:

$$a := 0.0648 \quad \text{m} \quad \text{radius of driver}$$

$$\rho_0 := 1.18 \quad \text{kg/m}^3 \quad \text{density of air}$$

$$M_{m1} := 2.67 \cdot a^3 \cdot \rho_0 \quad \text{air load mass on the two sides of the diaphragm}$$

$$M_{m1} = 8.573 \cdot 10^{-4}$$

$$M_{md} := \frac{M}{\left(\frac{F_s}{F_{sp}}\right)^2 - 1} - M_{m1}$$

$$M_{md} = 0.015 \quad \text{kg}$$

Voice Coil Inductance Using Z @ 1500 Hz and 10000 Hz:

$$f1 := 1500 \quad Z1 := 5.9984 \quad \text{Ohms}$$

$$\omega1 := 2 \cdot \pi \cdot f1$$

$$f2 := 10008 \quad Z2 := 16.1140 \quad \text{Ohms}$$

$$\omega2 := 2 \cdot \pi \cdot f2$$

$$L_e = \sqrt{\frac{Z2^2 - Z1^2}{\omega2^2 - \omega1^2}}$$

$$L_e = 2.406 \cdot 10^{-4} \quad \text{H}$$

## APPENDIX B

### LUMPED PARAMETER EQUIVALENT CIRCUIT NETLIST

```
7th Order Bandpass System
*FILE: FIG2_4.CIR
VEG 0 1 AC 2.0V
R1 1 0 1K
EEG1 2 0 1 0 1.0
EEG2 8 0 1 0 1.0
RC1 2 3 0.75
LC1 3 4 0.0015
RE1 4 5 3.62
LE1 5 6 0.26E-3
RC2 8 9 0.75
LC2 9 10 0.0015
RE2 10 11 3.55
LE2 11 12 0.24E-3
HBLU1 6 7 VD3 4.0684
HBLU2 12 13 VD3 4.2118
VD1 7 0 AC 0V
VD2 13 0 AC 0V
HBLI1 15 14 VD1 4.0684
HBLI2 14 0 VD2 4.2118
RMS 15 16 1.0655
LMS 16 17 0.0145
CMS 17 18 532.6E-6
ESDP 18 19 22 20 0.0132
VD3 19 0 AC 0V
FSDU 20 22 VD3 0.0132
LMATL 20 21 56.9
CABL 20 0 290N
RALL 20 0 500K
VD4 21 0 AC 0V
CABH 22 0 62N
RALH 22 0 500K
LMATH 22 23 53.3
VD5 23 0 AC 0V
FS1 0 24 VD4 1.0
FS2 0 24 VD5 1.0
VSUM 24 0 AC 0V
.AC DEC 50 10 10K
.PROBE
.END
```

## APPENDIX C

### MATHCAD CALCULATIONS FOR THE ENCLOSURE

Enclosure Design

One Dual Voice Coil Driver, 7th Order Bandpass

Acoustic Components from the Preliminary Equivalent Circuit (fig4.cir):

$$CABL := 290 \cdot 10^{-9} \quad \text{m}^5/\text{N}$$

$$LMATL := 56.9 \quad \text{kg}/\text{m}^4$$

$$CABH := 62 \cdot 10^{-9} \quad \text{m}^5/\text{N}$$

$$LMATH := 53.3 \quad \text{kg}/\text{m}^4$$

Properties of Air: from Beranek [6], p.10

$$\rho := 1.18 \quad \text{kg}/\text{m}^3 \quad \text{Density of Air}$$

$$c := 344.5 \quad \text{m}/\text{s} \quad \text{Speed of Sound in Air}$$

Effective Piston Area of Driver

$$Sd := 0.0132 \quad \text{m}^2$$

1. Mounting Plate

Driver OD = 6.5 in, Choose Plate Dimensions 12x12 inches Square.

$$Imp := 12 \quad \text{in}$$

$$Amp := Imp^2$$

2. Rear Volume

$$Vabl := CABL \cdot \rho \cdot c^2$$

$$Vabl = 0.041 \quad \text{m}^3$$

$$Vabl := Vabl \cdot \left( \frac{100}{2.54} \right)^3 \quad (\text{converts m}^3 \text{ to in}^3)$$

$$Vabl = 2.478 \cdot 10^3 \quad \text{in}^3$$

Volume of Driver:

$$Vd := \frac{\pi \cdot 4^2}{4} \cdot (2.5) \quad (\text{approximately 4"dia by 2.5" deep})$$

$$Vd = 31.416 \quad \text{in}^3$$

Rear Volume Total:

$$Vrear := Vabl + Vd$$

$$Vrear = 2.51 \cdot 10^3 \quad \text{in}^3$$

$$L_{\text{rear}} = \frac{V_{\text{rear}}}{\text{Amp}}$$

$$L_{\text{rear}} = 17.429 \text{ in} \quad (\text{length of rear volume})$$

### 3. Front Volume

$$V_{\text{abh}} := \text{CABH} \cdot \rho \cdot c^2$$

$$V_{\text{abh}} := V_{\text{abh}} \cdot \left(\frac{100}{2.54}\right)^3 \quad (\text{converts m}^3 \text{ to in}^3)$$

$$V_{\text{abh}} = 529.848 \text{ in}^3$$

$$L_{\text{front}} := \frac{V_{\text{abh}}}{\text{Amp}}$$

$$L_{\text{front}} = 3.679 \text{ in} \quad (\text{length of front volume})$$

### 4. Enclosure Mass Loading Calculations - from Leach [11]

$$L_{\text{rearm}} := \frac{L_{\text{rear}}}{39.37} \quad (\text{converts inches to meters})$$

$$S_b := \frac{\text{Amp}}{(39.37^2)} \quad (\text{converts square inches to square meters})$$

$$LMABL := \frac{\rho \cdot L_{\text{rearm}} \cdot S_d}{3 \cdot S_b^2} + \frac{8 \cdot \rho \cdot \left(1 - \frac{S_d}{S_b}\right)}{3 \cdot \pi \cdot \sqrt{\pi \cdot S_d}}$$

$$LMABL = 4.486 \quad \text{kg/m}^4$$

$$L_{\text{frontm}} := \frac{L_{\text{front}}}{39.37} \quad (\text{converts inches to meters})$$

$$LMABH := \frac{\rho \cdot L_{\text{frontm}} \cdot S_d}{3 \cdot S_b^2} + \frac{8 \cdot \rho \cdot \left(1 - \frac{S_d}{S_b}\right)}{3 \cdot \pi \cdot \sqrt{\pi \cdot S_d}}$$

$$LMABH = 4.276 \quad \text{kg/m}^4$$

### 5. Port Calculations

Choose Port Width = 0.75 inches

$$w_p := 0.75 \text{ in}$$

Height of the port is determined by the mounting plate.

$$h_p := l_{mp}$$

Port Area:

$$S_p := w_p \cdot h_p$$

$$S_p = 9 \quad \text{in}^2$$

$$S_p := S_p \cdot (645.16 \cdot 10^{-6}) \quad (\text{converts in}^2 \text{ to m}^2)$$

Effective Radius of Ports:

$$a := \sqrt{\frac{S_p}{\pi}} \quad a = 0.043 \quad \text{m}$$

Inner End Correction of Ports: see Beranek [6], p.133

$$l_{ecl} := 0.613 \cdot a$$

$$L_{MECL} := \frac{\rho \cdot l_{ecl}}{S_p} \quad L_{MECL} = 5.356 \quad \text{kg/m}^4$$

$$L_{MECH} := L_{MECL} \quad (\text{same effective radius and area})$$

Acoustic Radiation Impedance of Ports (same for both): from Beranek [6], p.121.

$$RA1 := \frac{0.1404 \cdot \rho \cdot c}{a^2} \quad RA1 = 3.088 \cdot 10^4 \quad \text{N}^* \text{s/m}^5$$

$$RA2 := \frac{\rho \cdot c}{\pi \cdot a^2} \quad RA2 = 7.001 \cdot 10^4 \quad \text{N}^* \text{s/m}^5$$

$$CA1 := \frac{5.94 \cdot a^3}{\rho \cdot c^2} \quad CA1 = 3.37 \cdot 10^{-9} \quad \text{m}^5/\text{N}$$

$$L_{MA1} := \frac{8 \cdot \rho}{3 \cdot \pi^2 \cdot a} \quad L_{MA1} = 7.416 \quad \text{kg/m}^4$$

Front Port Length:

$$L_{MAPH} := L_{MATH} - L_{MABH} - L_{MECH} - L_{MA1} \quad (\text{acoustic mass of air in the front port})$$

$$l_{pfi} := \frac{L_{MAPH} \cdot S_p}{\rho} \quad l_{pfi} = 0.178 \quad \text{m}$$

$$l_{pfi} := l_{pfi} \cdot (39.37) \quad (\text{converts meters to inches})$$

$$l_{pfi} = 7.023 \quad \text{in}$$

Rear Port Length:

$$\text{LMAPL} := \text{LMATL} - \text{LMABL} - \text{LMECL} - \text{LMA1} \quad (\text{acoustic mass of air in the rear port})$$

$$l_{\text{prm}} := \frac{\text{LMAPL} \cdot S_p}{\rho} \quad l_{\text{prm}} = 0.195 \quad \text{m}$$

$$l_{\text{pri}} := l_{\text{prm}} \cdot (39.37) \quad (\text{converts meters to inches})$$

$$l_{\text{pri}} = 7.68 \quad \text{in}$$

Resonant Port Calculations

Use  $n := 3$  subdivisions.

Front Port:

$$l_{\text{rpf}} := \frac{l_{\text{pfm}}}{n}$$

$$v_{\text{rpf}} := S_p \cdot l_{\text{rpf}}$$

$$L_{\text{mrph}} := \frac{\rho \cdot l_{\text{rpf}}}{S_p}$$

$$C_{\text{aph}} := \frac{v_{\text{rpf}}}{\rho \cdot c^2}$$

Front Resonant Port Components:

$$\text{LMRPH1} := \frac{L_{\text{mrph}}}{2} \quad \text{LMRPH1} = 6.042 \quad \text{kg/m}^4$$

$$\text{LMRPH2} := L_{\text{mrph}} \quad \text{LMRPH2} = 12.084 \quad \text{kg/m}^4$$

$$\text{LMRPH3} := L_{\text{mrph}} \quad \text{LMRPH3} = 12.084 \quad \text{kg/m}^4$$

$$\text{LMRPH4} := \frac{L_{\text{mrph}}}{2} \quad \text{LMRPH4} = 6.042 \quad \text{kg/m}^4$$

$$\text{CAPH1} := C_{\text{aph}} \quad \text{CAPH1} = 2.465 \cdot 10^{-9} \quad \text{m}^5/\text{N}$$

$$\text{CAPH2} := C_{\text{aph}} \quad \text{CAPH2} = 2.465 \cdot 10^{-9} \quad \text{m}^5/\text{N}$$

$$\text{CAPH3} := C_{\text{aph}} \quad \text{CAPH3} = 2.465 \cdot 10^{-9} \quad \text{m}^5/\text{N}$$

Rear Port:

$$l_{\text{rpr}} := \frac{l_{\text{prm}}}{n}$$

$$vrpr := Sp \cdot lrpr$$

$$Lmrpl := \frac{\rho \cdot lrpr}{Sp}$$

$$Capl := \frac{vrpr}{\rho \cdot c^2}$$

Rear Resonant Port Components:

$$LMRPL1 := \frac{Lmrpl}{2} \quad LMRPL1 = 6.607 \quad \text{kg/m}^4$$

$$LMRPL2 := Lmrpl \quad LMRPL2 = 13.214 \quad \text{kg/m}^4$$

$$LMRPL3 := Lmrpl \quad LMRPL3 = 13.214 \quad \text{kg/m}^4$$

$$LMRPL4 := \frac{Lmrpl}{2} \quad LMRPL4 = 6.607 \quad \text{kg/m}^4$$

$$CAPL1 := Capl \quad CAPL1 = 2.696 \cdot 10^{-9} \quad \text{m}^5/\text{N}$$

$$CAPL2 := Capl \quad CAPL2 = 2.696 \cdot 10^{-9} \quad \text{m}^5/\text{N}$$

$$CAPL3 := Capl \quad CAPL3 = 2.696 \cdot 10^{-9} \quad \text{m}^5/\text{N}$$

## 6. Resonant Volume Calculations

Use  $n := 3$  Subdivisions

Front Volume:

$$Sb = 0.093 \quad \text{m}^2 \quad (\text{inside area of the enclosure})$$

$$Lfm := \frac{Lfront}{39.37}$$

$$Lfsect := \frac{Lfm}{n}$$

$$Vfsect := Lfsect \cdot Sb$$

$$Lcabh := \frac{\rho \cdot Vfsect}{Sb}$$

$$Cabh := \frac{Vfsect}{\rho \cdot c^2}$$

## Front Resonant Volume Components:

$$LCABH1 := \frac{Lcabh}{2} \quad LCABH1 = 0.198 \quad \text{kg/m}^4$$

$$LCABH2 := Lcabh \quad LCABH2 = 0.396 \quad \text{kg/m}^4$$

$$LCABH3 := Lcabh \quad LCABH3 = 0.396 \quad \text{kg/m}^4$$

$$LCABH4 := \frac{Lcabh}{2} \quad LCABH4 = 0.198 \quad \text{kg/m}^4$$

$$CABH1 := Cabh \quad CABH1 = 2.067 \cdot 10^{-8} \quad \text{m}^5/\text{N}$$

$$CABH2 := Cabh \quad CABH2 = 2.067 \cdot 10^{-8} \quad \text{m}^5/\text{N}$$

$$CABH3 := Cabh \quad CABH3 = 2.067 \cdot 10^{-8} \quad \text{m}^5/\text{N}$$

## Front Volume Correction Component:

$$tply := 0.465 \quad \text{in} \quad (1/2" \text{ plywood thickness})$$

$$Vrcor := (tply + wp) \cdot (lmp - lphi) \cdot lmp$$

$$Vrcor = 72.563 \quad \text{in}^3$$

$$Vrcor := Vrcor \cdot \left(\frac{2.54}{100}\right)^3 \quad (\text{converts in}^3 \text{ to m}^3)$$

$$CABH4 := \frac{Vrcor}{\rho \cdot c^2}$$

$$CABH4 = 8.491 \cdot 10^{-9} \quad \text{m}^5/\text{N}$$

## Rear Volume:

$$Lrm := Lrear \cdot \left(\frac{1}{39.37}\right) \quad (\text{converts inches to meters})$$

$$Sb = 0.093 \quad \text{m}^2 \quad (\text{inside area of the enclosure})$$

$$Lrsect := \frac{Lrm}{n}$$

$$Vrsect := Lrsect \cdot Sb$$



$$L_{cabl} := \frac{\rho \cdot L_{rsect}}{S_b}$$

$$Cabl := \frac{V_{rsect}}{\rho \cdot c^2}$$

Rear Resonant Volume Components:

$$LCABL1 := \frac{L_{cabl}}{2} \quad LCABL1 = 0.937 \quad \text{kg/m}^4$$

$$LCABL2 := L_{cabl} \quad LCABL2 = 1.874 \quad \text{kg/m}^4$$

$$LCABL3 := L_{cabl} \quad LCABL3 = 1.874 \quad \text{kg/m}^4$$

$$LCABL4 := \frac{L_{cabl}}{2} \quad LCABL4 = 0.937 \quad \text{kg/m}^4$$

$$CABL1 := Cabl \quad CABL1 = 9.789 \cdot 10^{-8} \quad \text{m}^5/\text{N}$$

$$CABL2 := Cabl \quad CABL2 = 9.789 \cdot 10^{-8} \quad \text{m}^5/\text{N}$$

$$CABL3 := Cabl \quad CABL3 = 9.789 \cdot 10^{-8} \quad \text{m}^5/\text{N}$$

Rear Volume Correction Component:

$$t_{ply} := 0.465 \quad \text{in} \quad (\text{plywood thickness})$$

$$l_{offset} := 2.89 \quad \text{in}$$

$$V_{rcor} := (t_{ply} + w_p) \cdot (L_{rear} - l_{pri} - l_{offset}) \cdot l_{mp}$$

$$V_{rcor} = 100.002 \quad \text{in}^3$$

$$V_{rcor} := V_{rcor} \cdot \left(\frac{2.54}{100}\right)^3 \quad (\text{converts in}^3 \text{ to m}^3)$$

$$CABL4 := \frac{V_{rcor}}{\rho \cdot c^2}$$

$$CABL4 = 1.17 \cdot 10^{-8} \quad \text{m}^5/\text{N}$$

### 7. Enclosure Leakage Resistances RALL, RALH

Set both front and rear resonance quality factors  $Q = 12$ : from Leach [11]

The high and low system resonant frequencies are:

$$f_h := \frac{1}{2 \cdot \pi \cdot \sqrt{L_{MATH} \cdot C_{ABH}}} \quad f_h = 87.551 \quad \text{Hz}$$

$$f_l := \frac{1}{2 \cdot \pi \cdot \sqrt{L_{MATL} \cdot C_{ABL}}} \quad f_l = 39.18 \quad \text{Hz}$$

Let

$$Q_h := 12 \quad \text{and} \quad Q_l := 12$$

Then

$$R_{ALH} := \frac{Q_h}{2 \cdot \pi \cdot f_h \cdot C_{ABH}} \quad R_{ALH} = 3.518 \cdot 10^5 \quad \text{N*s/m}^5$$

and

$$R_{ALL} := \frac{Q_l}{2 \cdot \pi \cdot f_l \cdot C_{ABL}} \quad R_{ALL} = 1.681 \cdot 10^5 \quad \text{N*s/m}^5$$

### 8. Final Enclosure Inside Dimensions

$$V_{abh} := C_{ABH} \cdot \rho \cdot c^2 \cdot \left( \frac{100}{2.54} \right)^3 + (t_{ply} + w_p) \cdot h_p \cdot l_p f_i$$

$$L_{frontf} := \frac{V_{abh}}{\text{Amp}}$$

$$L_{frontf} = 4.391 \quad \text{in}$$

$$L_{rear} = 17.429 \quad \text{in}$$

## APPENDIX D

### COMPLETE EQUIVALENT CIRCUIT NETLIST

7th Order Bandpass System  
\*FILE: FIG2\_7.CIR  
\*Distributed Element Ports and Enclosure Volumes  
VEG 0 1 AC 2.0V  
R1 1 0 1K  
EEG1 2 0 1 0 1.0  
EEG2 8 0 1 0 1.0  
RC1 2 3 0.75  
LC1 3 4 0.0015  
RE1 4 5 3.62  
LE1 5 6 0.26E-3  
RC2 8 9 0.75  
LC2 9 10 0.0015  
RE2 10 11 3.55  
LE2 11 12 0.24E-3  
HBLU1 6 7 VD3 4.0684  
HBLU2 12 13 VD3 4.2118  
VD1 7 0 AC 0V  
VD2 13 0 AC 0V  
HBLI1 15 14 VD1 4.0684  
HBLI2 14 0 VD2 4.2118  
RMS 15 16 1.0655  
LMS 16 17 0.0145  
CMS 17 18 532.6E-6  
ESDP 18 19 36 20 0.0132  
VD3 19 0 AC 0V  
FSDU 20 36 VD3 0.0132  
LMABL 20 21 4.486  
LCABL1 21 22 0.937  
CABL1 22 25 97.89N  
LCABL2 22 23 1.874  
CABL2 23 25 97.89N  
LCABL3 23 24 1.874  
CABL3 24 25 97.89N  
LCABL4 24 26 0.937  
CABL4 26 25 11.71N  
VD8 25 35 AC 0V  
RALL 26 35 168K  
LMECL 26 27 5.356

LMRPL1 27 28 6.607  
CAPL1 28 31 2.696N  
LMRPL2 28 29 13.214  
CAPL2 29 31 2.696N  
LMRPL3 29 30 13.214  
CAPL3 30 31 2.696N  
LMRPL4 30 32 6.607  
VD6 31 35 AC 0V  
RA1L 32 33 30.88K  
RA2L 33 34 70.01K  
CA1L 32 33 3.37N  
LMAIL 32 34 7.416  
VD4 34 35 AC 0V  
VD10 35 0 AC 0V  
LMABH 36 37 4.276  
LCABH1 37 38 0.198  
CABH1 38 41 20.67N  
LCABH2 38 39 0.396  
CABH2 39 41 20.67N  
LCABH3 39 40 0.396  
CABH3 40 41 20.67N  
LCABH4 40 42 0.198  
CABH4 42 41 8.491N  
VD9 41 51 AC 0V  
RALH 42 51 352K  
LMECH 42 43 5.356  
LMRPH1 43 44 6.042  
CAPH1 44 47 2.465N  
LMRPH2 44 45 12.084  
CAPH2 45 47 2.465N  
LMRPH3 45 46 12.084  
CAPH3 46 47 2.465N  
LMRPH4 46 48 6.042  
VD7 47 51 AC 0V  
RA1H 48 49 30.88K  
RA2H 49 50 70.01K  
CA1H 48 49 3.37N  
LMA1H 48 50 7.416  
VD5 50 51 AC 0V  
VD11 51 0 AC 0V  
FS1 0 52 VD4 1.0  
FS2 0 52 VD5 1.0  
VPORTS 52 0 AC 0V  
FS3 0 53 VD6 1.0

```
FS4 0 53 VD7 1.0
VPVOL 53 0 AC 0V
FS5 0 54 VD8 1.0
FS6 0 54 VD9 1.0
VEVOL 54 0 AC 0V
FINT1 0 55 VD3 1.0
CINT1 55 0 1.0
RTINT1 55 0 100MEG
.AC DEC 50 10 10K
.PROBE
.END
```

# APPENDIX E

## MECHANICAL DRAWING OF THE ENCLOSURE

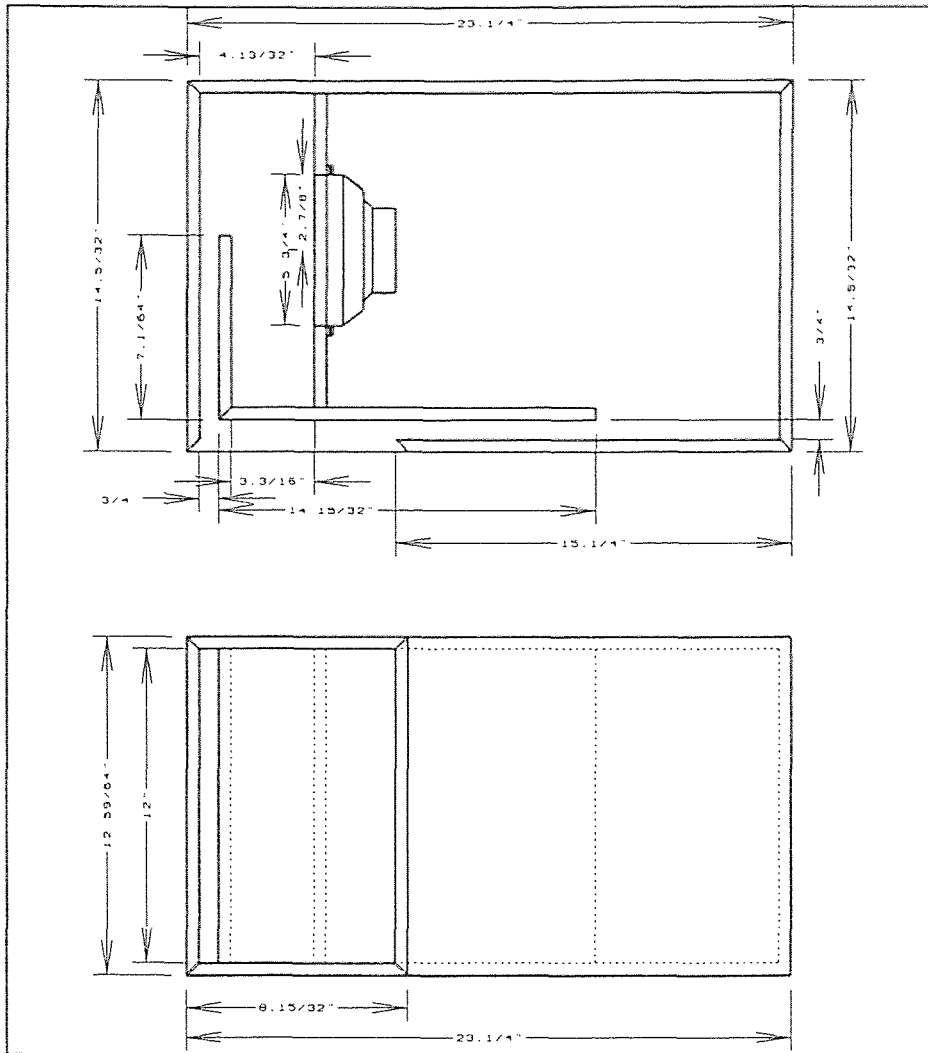


Figure E.1 Mechanical Drawing of the Enclosure

## APPENDIX F

### TEST SET DATA ACQUISITION PROGRAM LISTING

This program was written in Microsoft QuickBASIC version 4.5.

```
REM spltest9.bas 4/18/97
REM CALIBRATED WITH B&K TYPE 4230 SOUND LEVEL CALIBRATOR
REM MICROPHONE #1
REM SPL CALIBRATION FACTOR CHANGED TO 6.2661
REM MICROPHONE #2
REM SPL CALIBRATION FACTOR: CHANGE TO 11.3460
REM B&K MICROPHONE/PREAMP
REM SPL CALIBRATION FACTOR: CHANGE TO 6.5345
REM
DIM F(10000): DIM SPL(10000)
OPEN "SPLTEST9.DAT" FOR OUTPUT AS #1
P = 640
REM
1 CLS
PRINT "SELECT MICROPHONE CALIBRATION:"
PRINT "1 = MICROPHONE #1"
PRINT "2 = MICROPHONE #2"
PRINT "3 = B&K MICROPHONE/PREAMP"
PRINT
INPUT "WHICH MICROPHONE IS CONNECTED? "; M
IF M = 1 THEN
    CALFAC = 6.2661
ELSEIF M = 2 THEN
    CALFAC = 11.346
ELSEIF M = 3 THEN
    CALFAC = 6.5345
ELSE
    PRINT "SELECTION OUT OF RANGE: HIT ANY KEY TO CONTINUE:"
    GOTO 1
END IF
PRINT "CALFAC = "; CALFAC
REM DELAY LOOP
FOR I = 1 TO 100000
NEXT I
CLS
PRINT "Connect input 0 to ground and press <ENTER>";
```

```

INPUT T
OUT P, 0: D = INP(P): H = INP(P + 1): L = INP(P)
FOR C = 1 TO 100: NEXT C
OF = (H * 256 + L) * 5 / 4095
PRINT "OFFSET = "; OF
PRINT "TYPE ANY KEY TO CONTINUE"
1000
IF INKEY$ = "" THEN GOTO 1000
CLS
VMOS = 0
REM -----A/D READINGS-----
REM
REM -----PRE-TRIGGERING-----
DO
  OUT P, 0: D = INP(P)
  H = INP(P + 1)
  L = INP(P)
  VF = ((L + (H * 256)) * 5 / 4095 - OF)
  F1 = 7.955 + 34.411 * VF - 58.735 * VF ^ 2 + 94.456 * VF ^ 3 - 44.901 * VF ^ 4
  + 10.877 * VF ^ 5
  PRINT F1
LOOP UNTIL F1 >= 9.9
REM -----READ 10,000 POINTS-----

FOR I = 1 TO 10000
  OUT P, 0: D = INP(P)
  H = INP(P + 1)
  L = INP(P)
  VF = ((L + (H * 256)) * 5 / 4095 - OF)
  IF VF <= 2.984127 THEN
    F(I) = 7.955 + 34.411 * VF - 58.735 * VF ^ 2 + 94.456 * VF ^ 3 - 44.901 * VF ^
4 + 10.877 * VF ^ 5
  ELSE
    F(I) = -97960.937000000001# + 99785.331999999999# * VF - 36403.691# * VF ^
2 + 5425.926 * VF ^ 3 - 236.265 * VF ^ 4
  END IF
  OUT P, 1: D = INP(P)
  H = INP(P + 1)
  L = INP(P)
  VM = ((L + (H * 256)) * 5 / 4095 - OF)
  IF (VM - VMOS) <= 0 THEN SPL = 0: GOTO 10 ELSE
    SPL(I) = 20 * (LOG((VM - VMOS) / CALFAC) / LOG(10#)) + 110
    PRINT I, F(I), SPL(I)
  FOR C = 1 TO 1000: NEXT C

```



```

10 NEXT I
REM SAVE DATA
FOR I = 1 TO 10000
  PRINT #1, F(I), SPL(I)
NEXT I
REM
INPUT "DOMAIN? A=10-10Khz, B=20-20Khz ? ", D$
  IF D$ = "A" THEN 100 ELSE 200
REM
REM
100 REM 10-10K PLOT -----10 - 10K PLOT-----
CLS : SCREEN 9
REM=====GRAPH=====
REM
REM -----GRAPH LABELS-----
REM Y-AXIS:
PRINT "110 dB": PRINT : PRINT : PRINT : PRINT : PRINT : PRINT : PRINT :
PRINT
PRINT : PRINT "dB SPL": PRINT : PRINT : PRINT : PRINT : PRINT : PRINT :
PRINT
PRINT : PRINT : PRINT "40"
REM
REM X-AXIS:
PRINT TAB(7); "10"; TAB(30); "100"; TAB(53); "1000"; TAB(77); "10k"
PRINT TAB(40); "F (Hz)"
REM -----GRAPH AXES-----
REM
LINE (55, 290)-(620, 290): REM X-AXIS
LINE (55, 290)-(55, 10): REM Y-AXIS
REM -----Y-AXIS TIC MARKS (NOTE: 7 DIVISIONS, 40 EACH)-----
FOR K = 10 TO 290 STEP 40
  LINE (52, K)-(620, K), 13
NEXT K
REM
REM ----X-AXIS TICS, NOTE LOG SPACING AND CALCULATION OF SCALE
REM  CONSTANT-----
REM CALCULATE SCALING CONSTANT SC
REM XMX,XMN => MAX & MIN PIXEL POSITIONS OF X-AXIS
REM FMX,FMN => FREQUENCIES CORRESPONDING TO XMX,XMN
XMN = 55: XMX = 620: FMX = 10000: FMN = 10
SC = ((XMX - XMN) / (LOG(FMX / FMN) / LOG(10#)))
FOR K = 1 TO 28
  READ J

```

```

    LINE ((LOG(J / FMN) * SC) / LOG(10#) + XMN, 293)-((LOG(J / FMN) /
LOG(10#) * SC) + XMN, 10), 13
NEXT K
DATA
10,20,30,40,50,60,70,80,90,100,200,300,400,500,600,700,800,900,1000,2000,3000,4
000,5000,6000,7000,8000,9000,10000
REM
REM -----PLOT SPL(I) VS F(I)-----
REM
REM -----FIND N FOR F(10)-----
N = 1
WHILE F(N) < 10!
    N = N + 1
WEND
REM -----PLOT GRAPH-----
PSET (((LOG(F(N) / FMN) / LOG(10#)) * SC) + XMN, (290 - (SPL(N) - 40) * 4))
FOR I = N + 1 TO 10000
    IF SPL(I) < 40 THEN SPL(I) = 40
    IF F(I) <= 10000 THEN LINE -(((LOG(F(I) / FMN) / LOG(10#)) * SC) + XMN,
(290 - (SPL(I) - 40) * 4))
NEXT I
2000
IF INKEY$ = "" GOTO 2000
GOTO 4000
REM
200 REM 20-20K PLOT -----20-20K PLOT-----
CLS : SCREEN 9
REM=====GRAPH=====
REM
REM -----GRAPH LABELS-----
REM Y-AXIS:
PRINT "110 dB": PRINT : PRINT : PRINT : PRINT : PRINT : PRINT : PRINT :
PRINT
PRINT : PRINT "dB SPL": PRINT : PRINT : PRINT : PRINT : PRINT : PRINT :
PRINT
PRINT : PRINT : PRINT "40"
REM
REM X-AXIS:
PRINT TAB(7); "20"; TAB(30); "200"; TAB(53); "2000"; TAB(77); "20k"
PRINT TAB(40); "F (Hz)"
REM
REM -----GRAPH AXES-----
REM
LINE (55, 290)-(620, 290): REM X-AXIS

```

```

LINE (55, 290)-(55, 10): REM Y-AXIS
REM -----Y-AXIS TIC MARKS (NOTE: 7 DIVISIONS, 40 EACH)-----
FOR K = 10 TO 290 STEP 40
    LINE (52, K)-(620, K), 13
NEXT K
REM
REM ----X-AXIS TICS, NOTE LOG SPACING AND CALCULATION OF SCALE
REM  CONSTANT-----
REM CALCULATE SCALING CONSTANT SC
REM XMX,XMN => MAX & MIN PIXEL POSITIONS OF X-AXIS
REM FMX,FMN => FREQUENCIES CORRESPONDING TO XMX,XMN
XMN = 55: XMX = 620: FMX = 20000: FMN = 20
SC = ((XMX - XMN) / (LOG(FMX / FMN) / LOG(10#)))
FOR K = 1 TO 28
    READ J
    LINE ((LOG(J / FMN) * SC) / LOG(10#) + XMN, 293)-((LOG(J / FMN) /
LOG(10#) * SC) + XMN, 10), 13
NEXT K
DATA
20,40,60,80,100,120,140,160,180,200,400,600,800,1000,1200,1400,1600,1800,2000,
4000,6000,8000,10000,12000,14000,16000,18000,20000
REM LAST LINE ON 20-20K PLOT:
LINE (620, 293)-(620, 10), 13
REM
REM -----PLOT SPL(I) VS F(I)-----
REM
REM -----FIND N FOR F(20)-----
N = 1
WHILE F(N) < 20!
    N = N + 1
WEND
REM -----PLOT GRAPH-----
PSET (((LOG(F(N) / FMN) / LOG(10#)) * SC) + XMN, (290 - (SPL(N) - 40) * 4))

FOR I = (N + 1) TO 10000
    IF SPL(I) < 40 THEN SPL(I) = 40
    LINE -(((LOG(F(I) / FMN) / LOG(10#)) * SC) + XMN, (290 - (SPL(I) - 40) * 4))
NEXT I
3000
IF INKEY$ = "" GOTO 3000
4000 CLOSE #1

```

APPENDIX G

FIRST THIRTY VIBRATION MODES OF THE ENCLOSURE

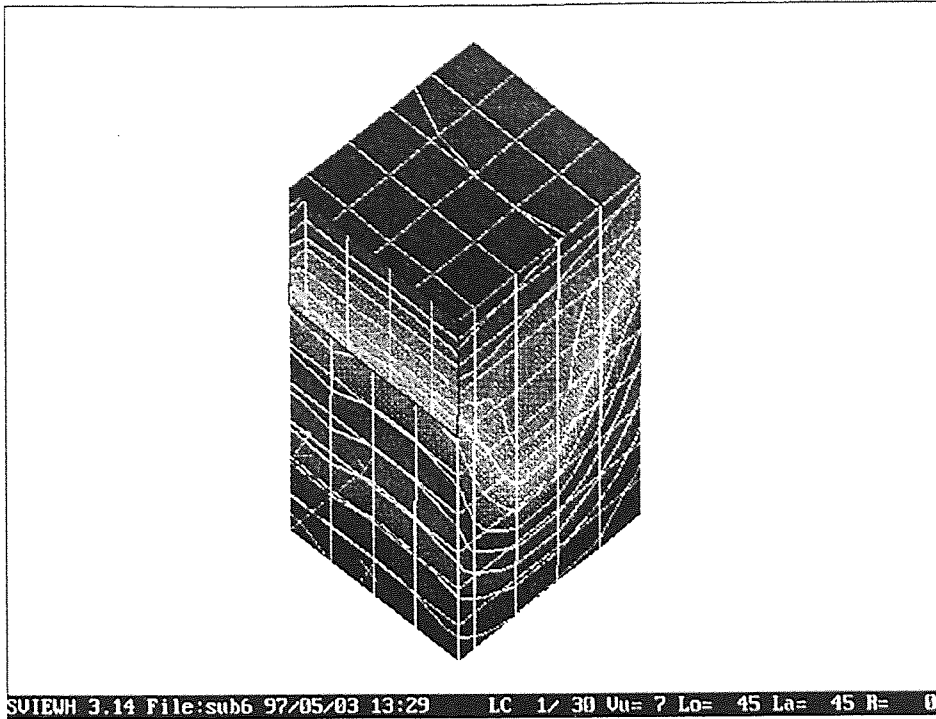


Figure G.1 Enclosure Mode Shape 1:  $f = 236.27$  Hz

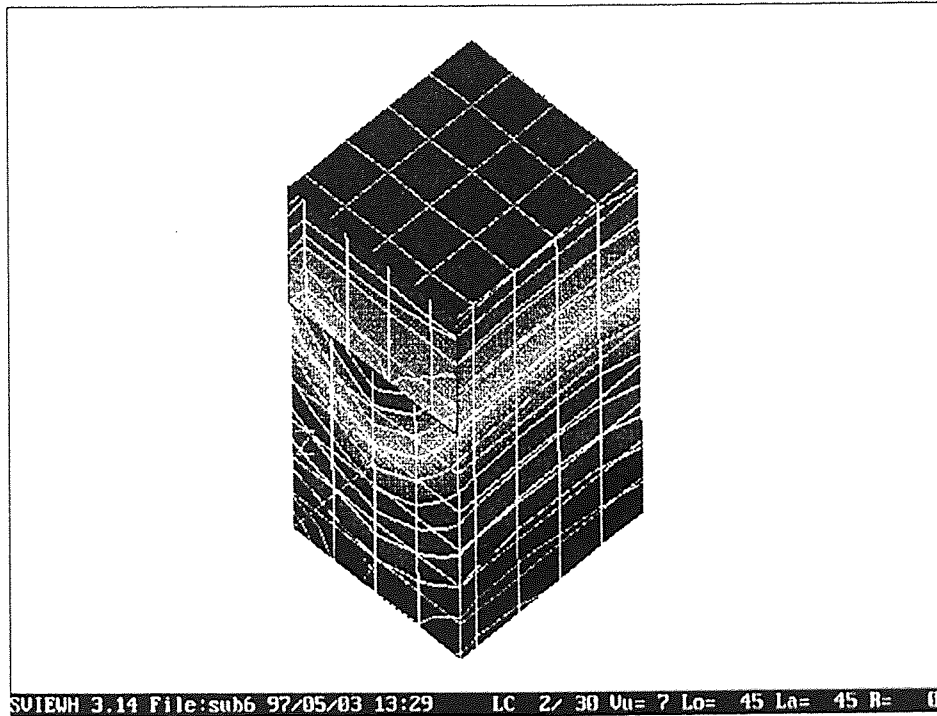
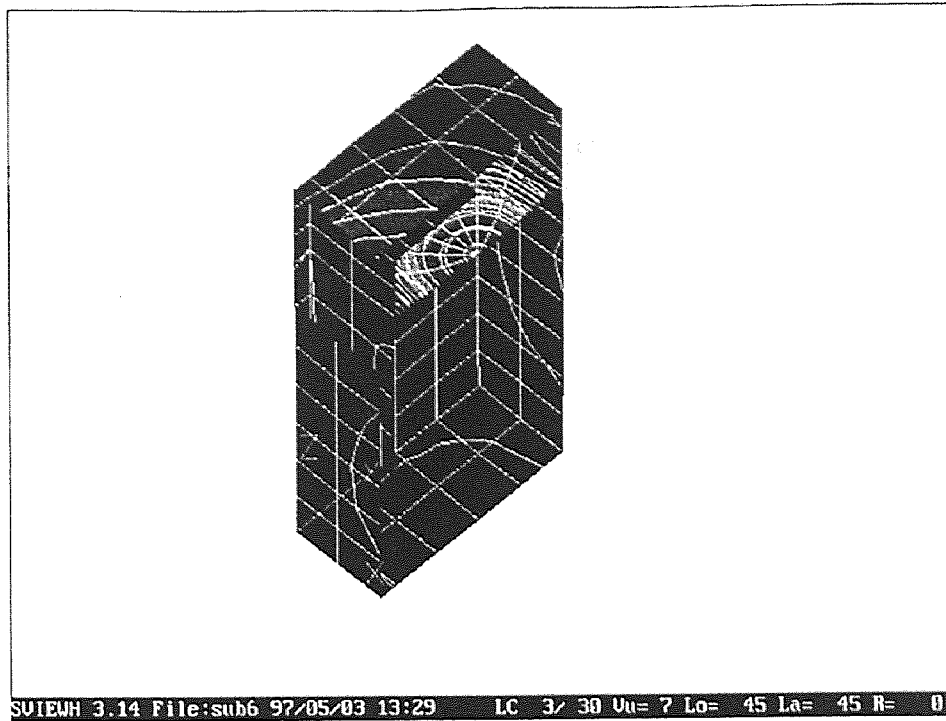
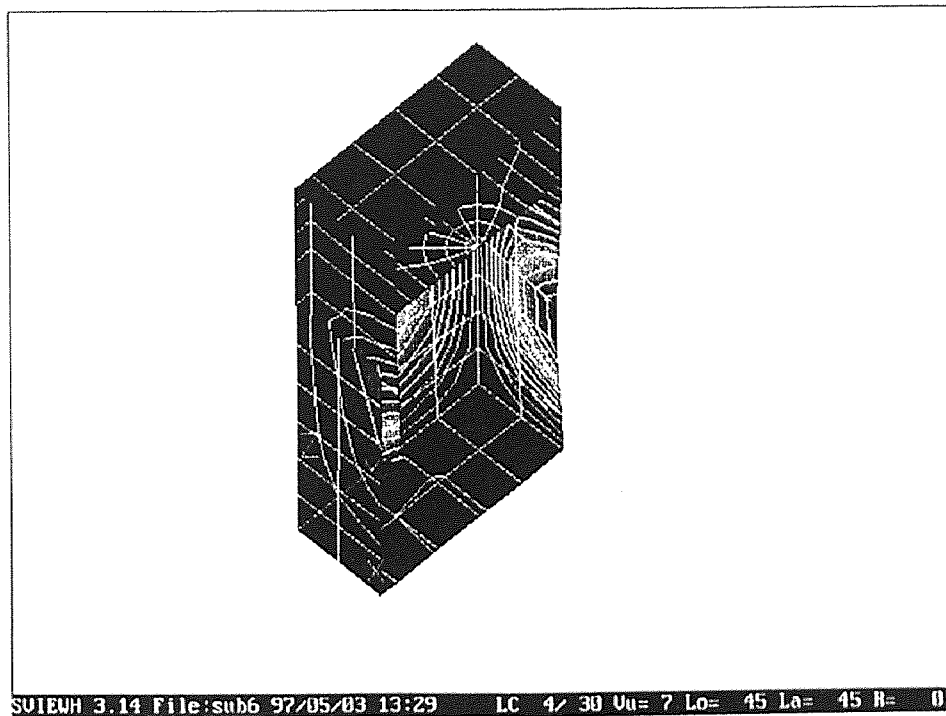


Figure G.2 Enclosure Mode Shape 2:  $f = 259.17$  Hz



**Figure G.3** Enclosure Mode Shape 3:  $f = 446.13$  Hz



**Figure G.4** Enclosure Mode Shape 4:  $f = 459.73$  Hz

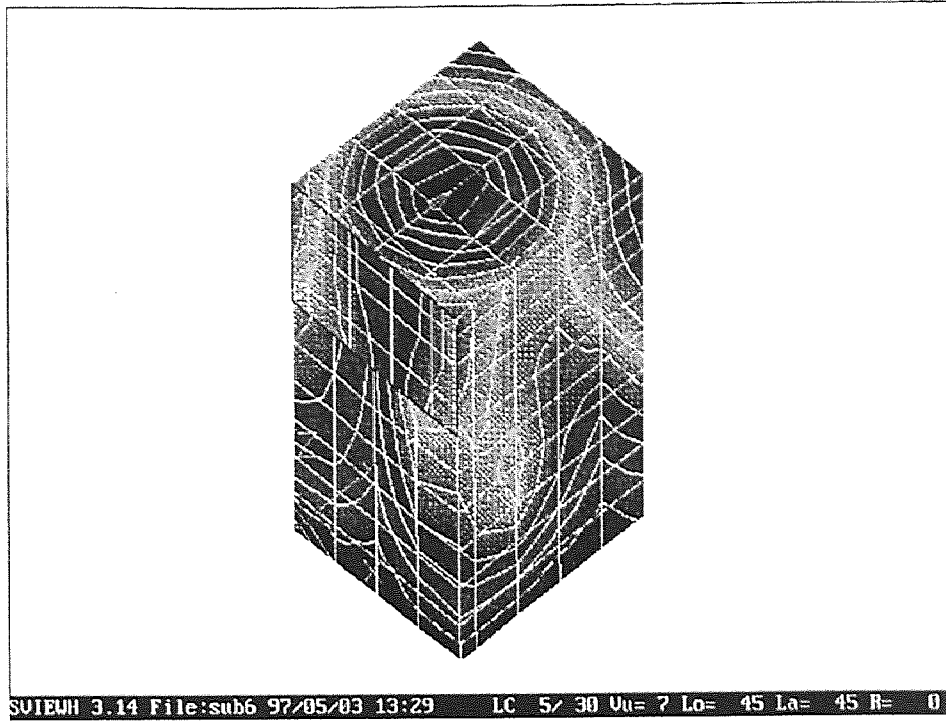


Figure G.5 Enclosure Mode Shape 5:  $f = 470.82$  Hz

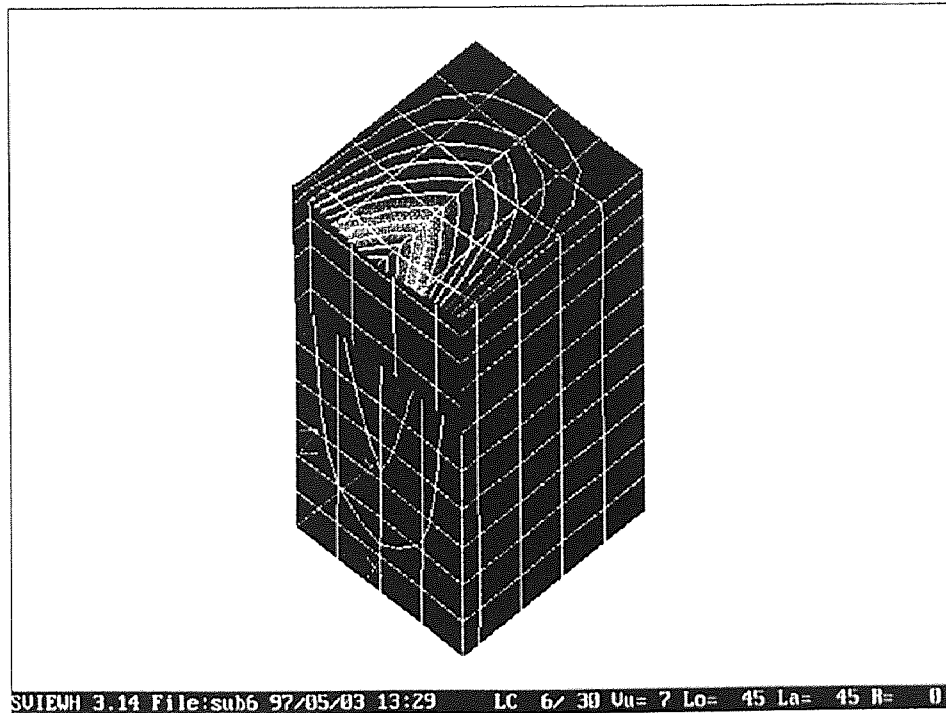


Figure G.6 Enclosure Mode Shape 6:  $f = 488.78$

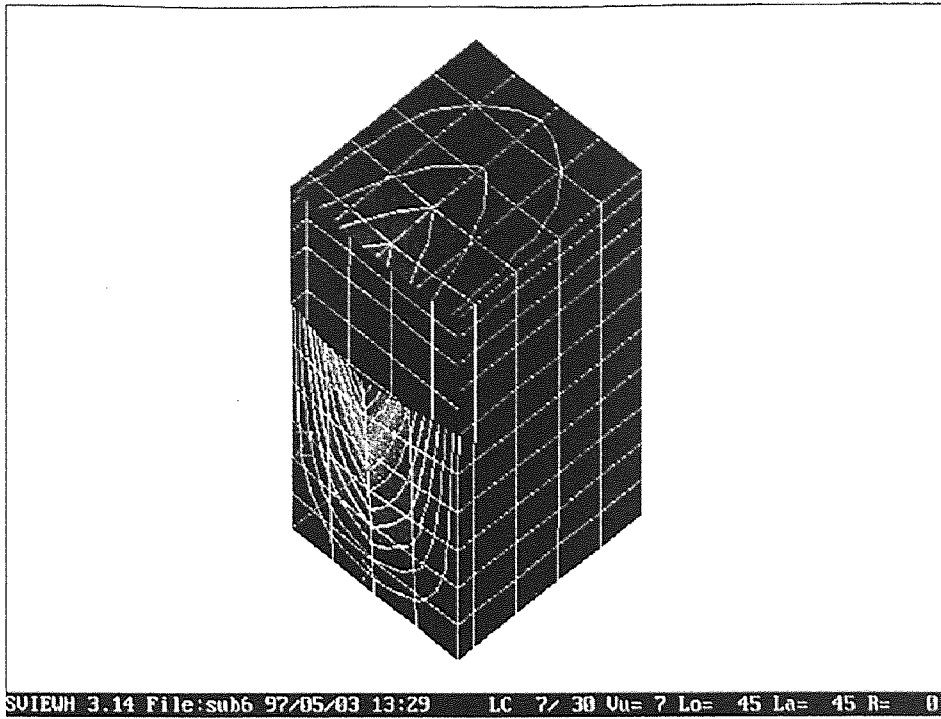


Figure G.7 Enclosure Mode Shape 7:  $f = 504.25$  Hz

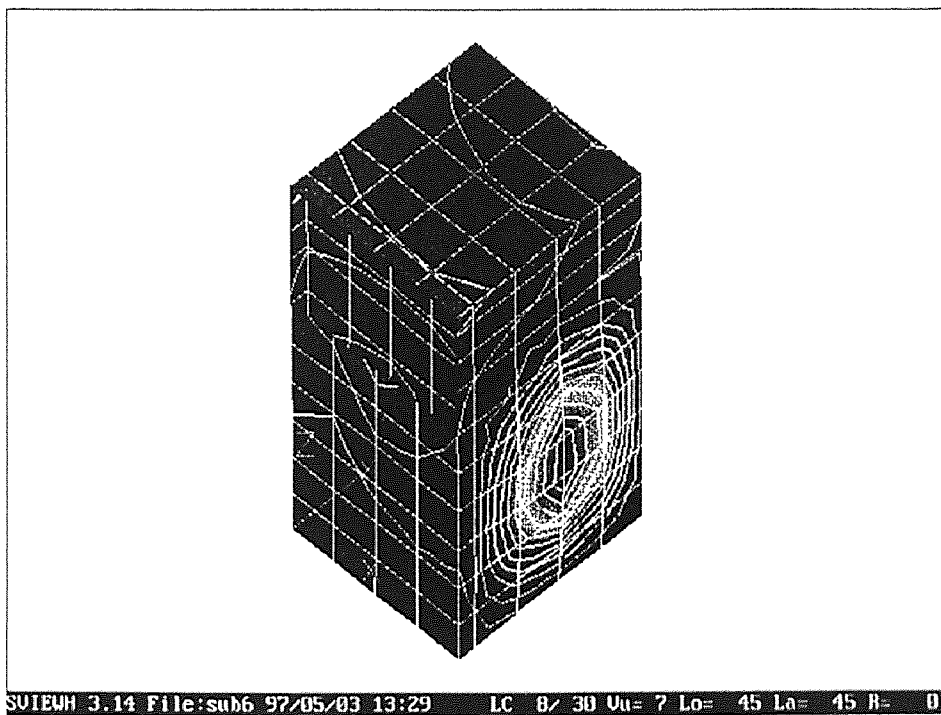


Figure G.8 Enclosure Mode Shape 8:  $f = 517.50$  Hz

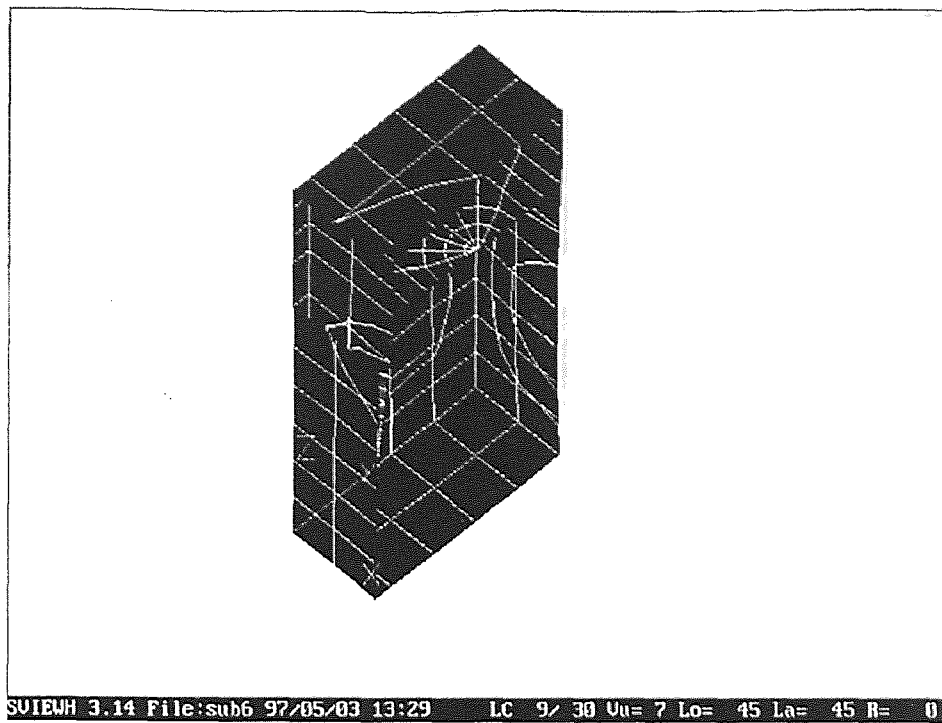


Figure G.9 Enclosure Mode Shape 9:  $f = 520.27$  Hz

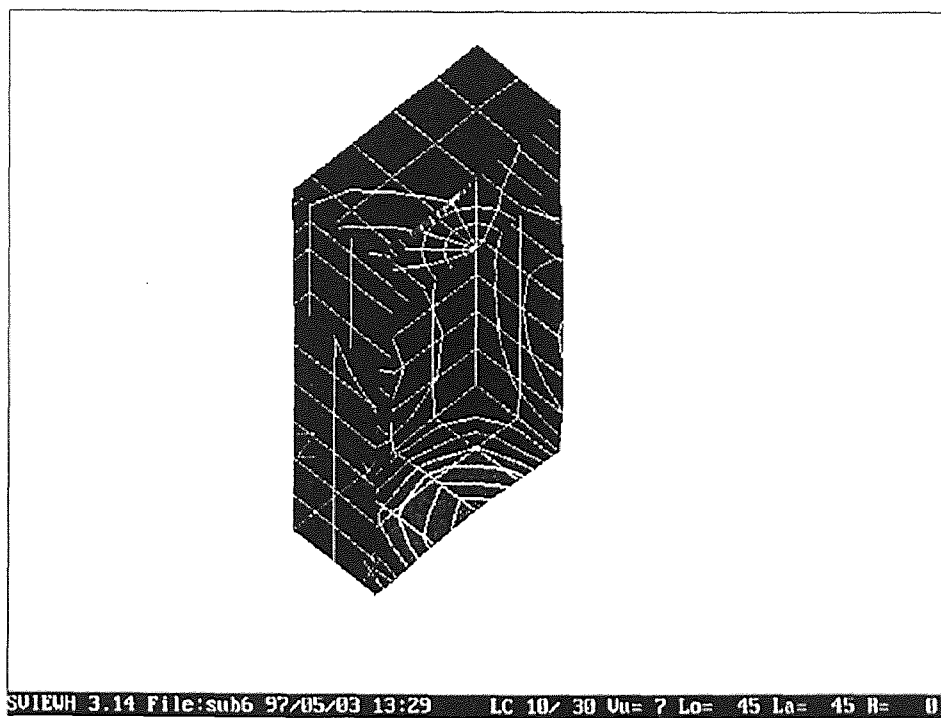


Figure G.10 Mode Shape 10:  $f = 575.61$  Hz



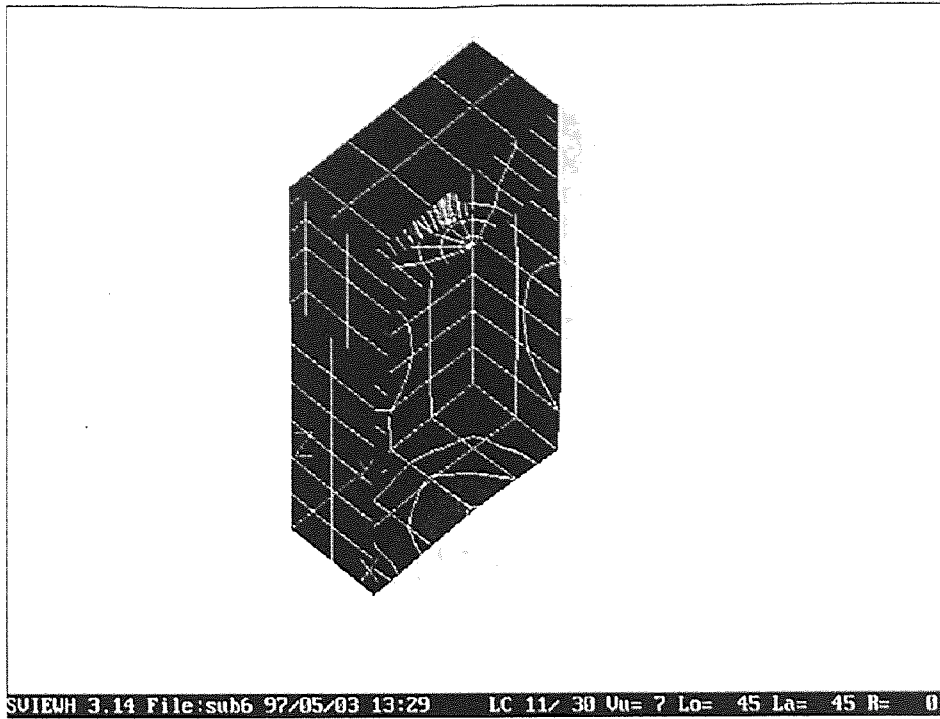


Figure G.11 Enclosure Mode Shape 11:  $f = 592.40$  Hz

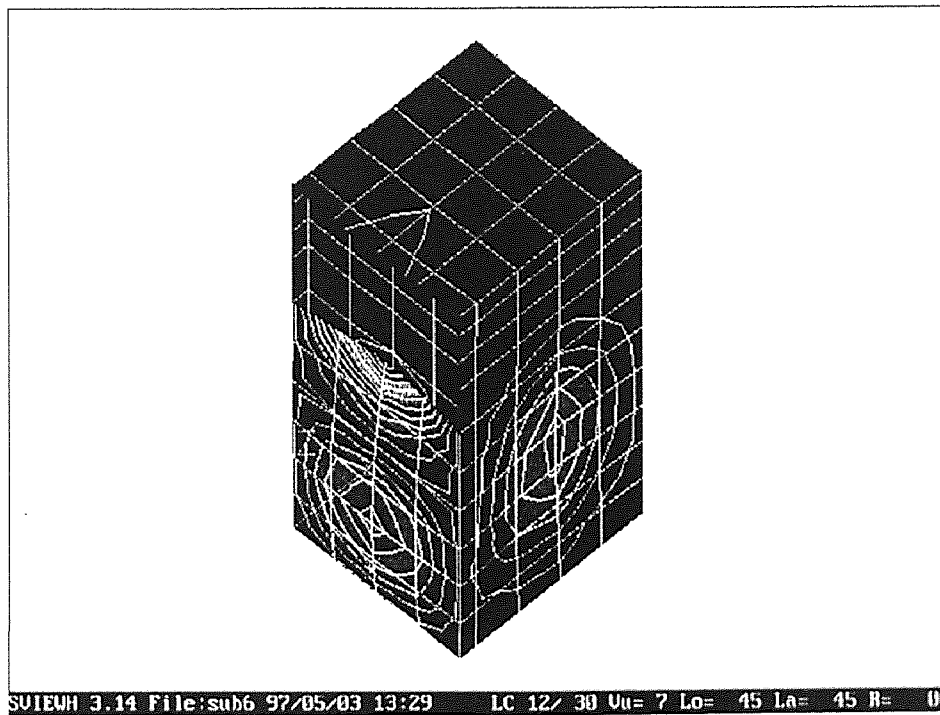


Figure G.12 Enclosure Mode Shape 12:  $f = 663.46$  Hz

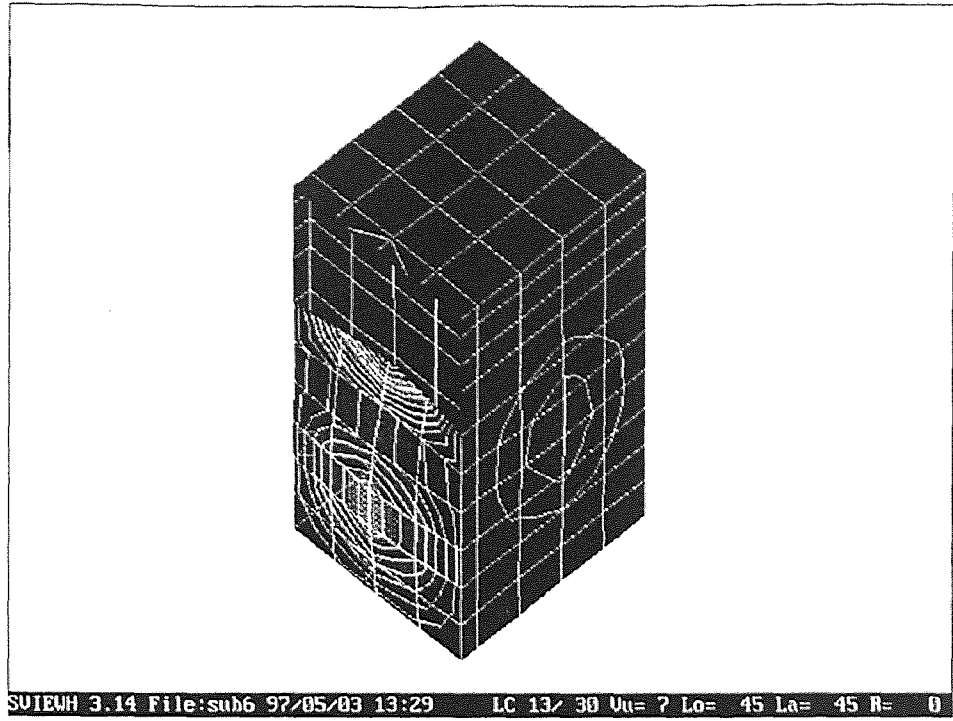


Figure G.13 Enclosure Mode 13:  $f = 730.33$  Hz

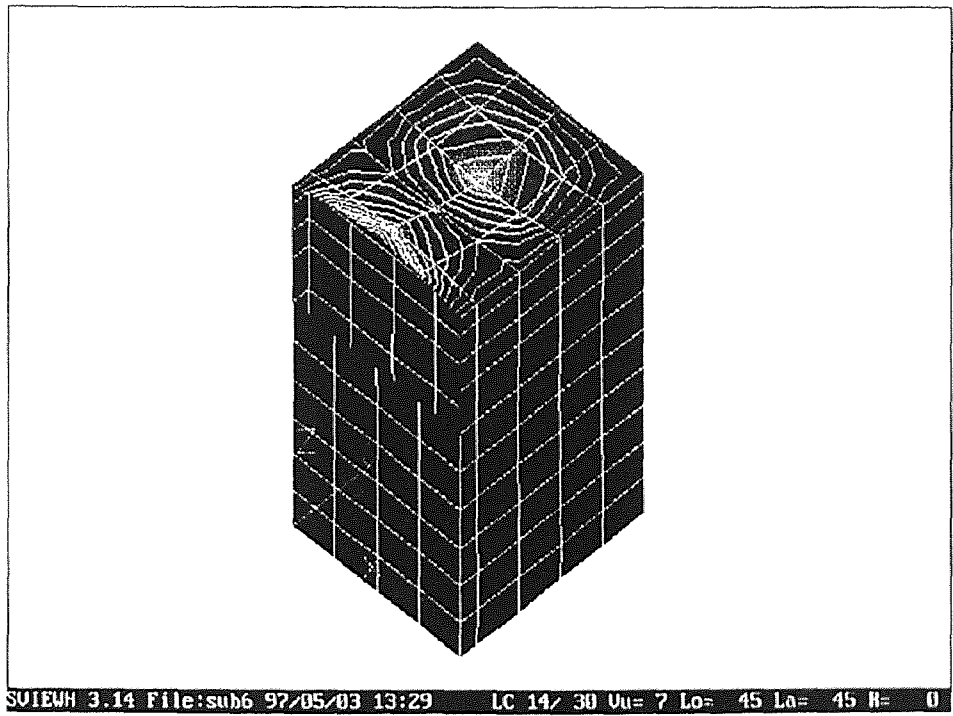


Figure G.14 Enclosure Mode 14:  $f = 766.32$  Hz

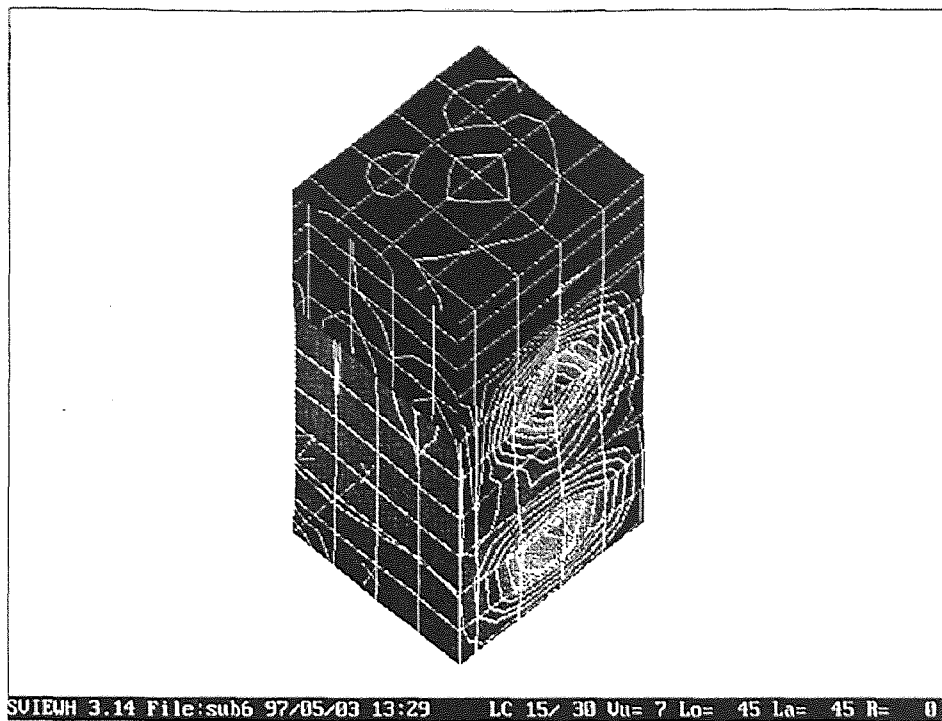


Figure G.15 Enclosure Mode Shape 15:  $f = 853.73$  Hz



Figure G.16 Enclosure Mode Shape 16:  $f = 870.25$  Hz

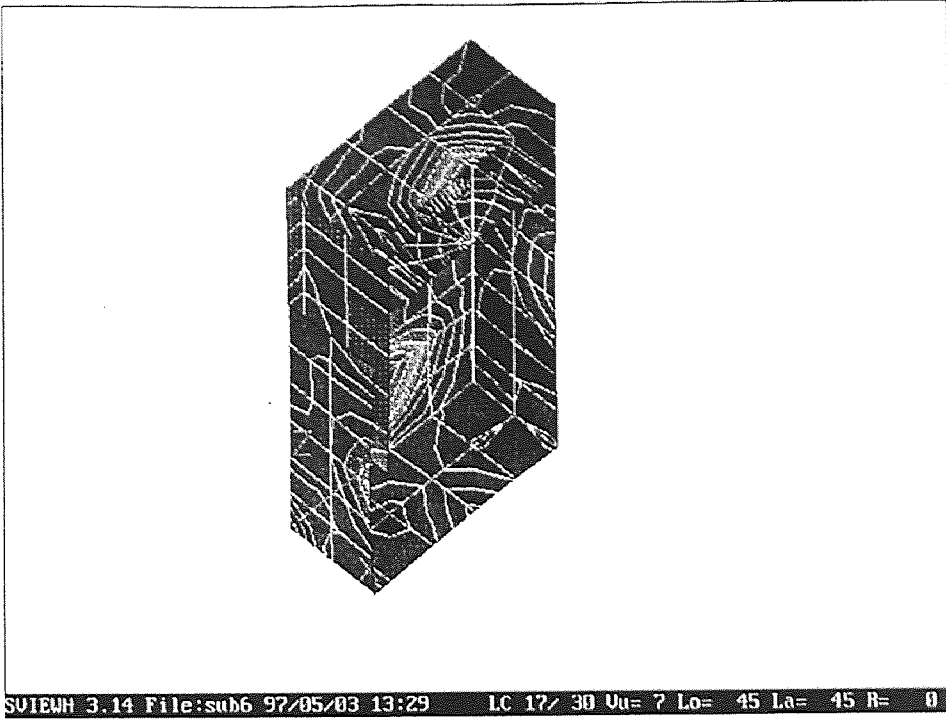


Figure G.17 Enclosure Mode Shape 17:  $f = 897.04$  Hz

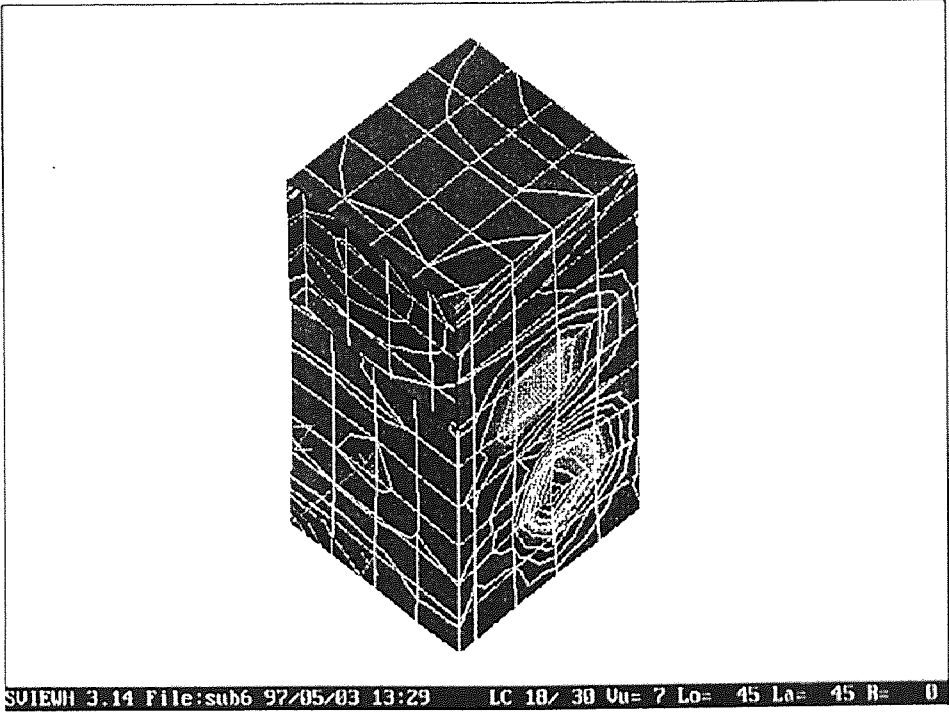


Figure G.18 Enclosure Mode Shape 18:  $f = 927.51$  Hz

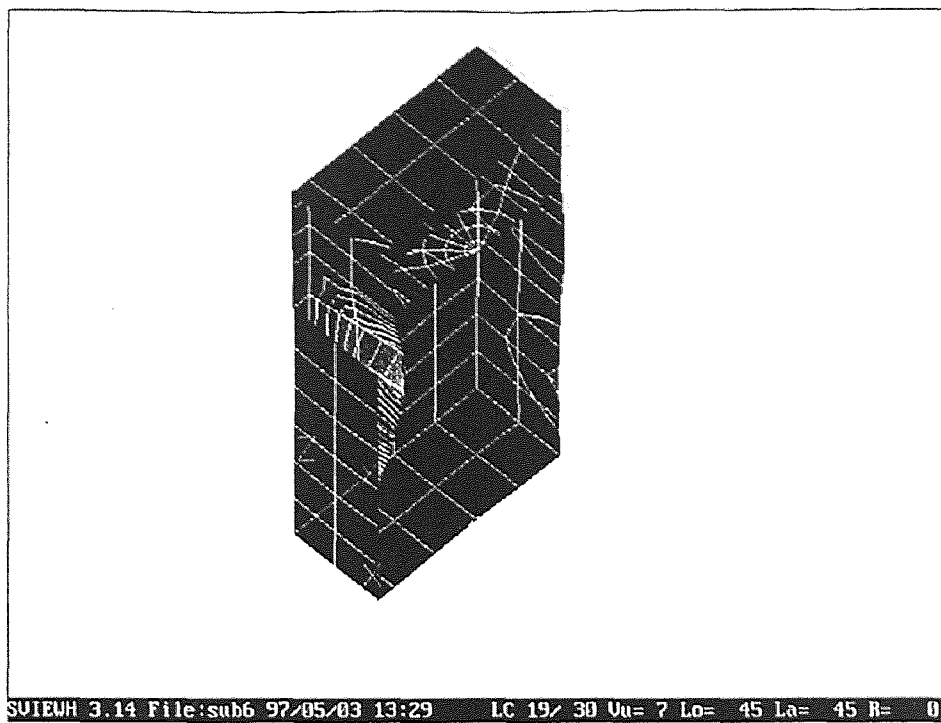


Figure G.19 Enclosure Mode 19:  $f = 941.49$  Hz

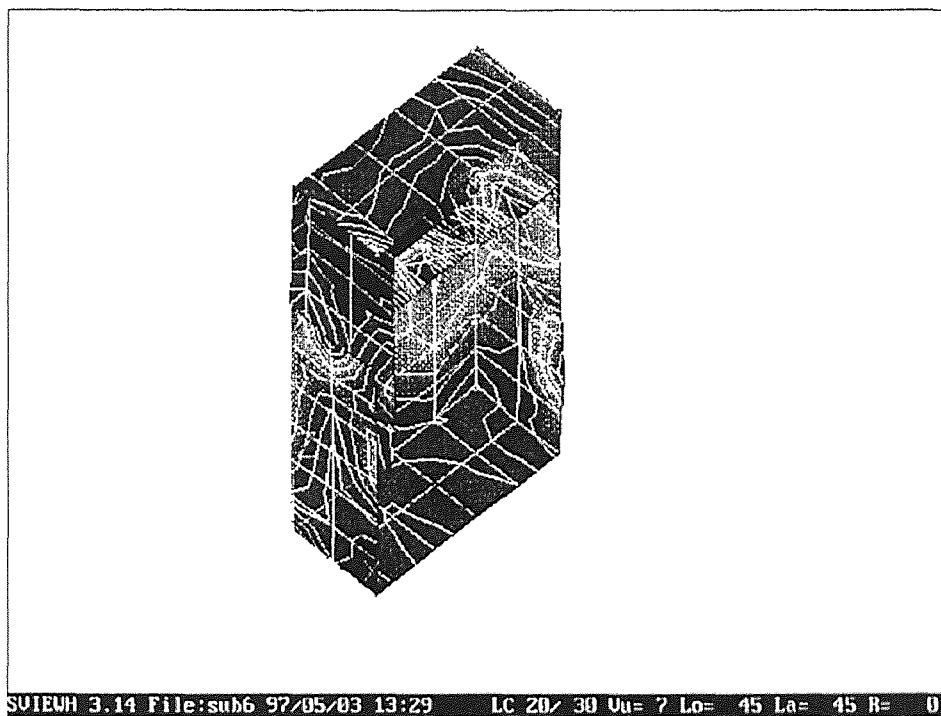


Figure G.20 Enclosure Mode Shape 20:  $f = 1018.9$  Hz

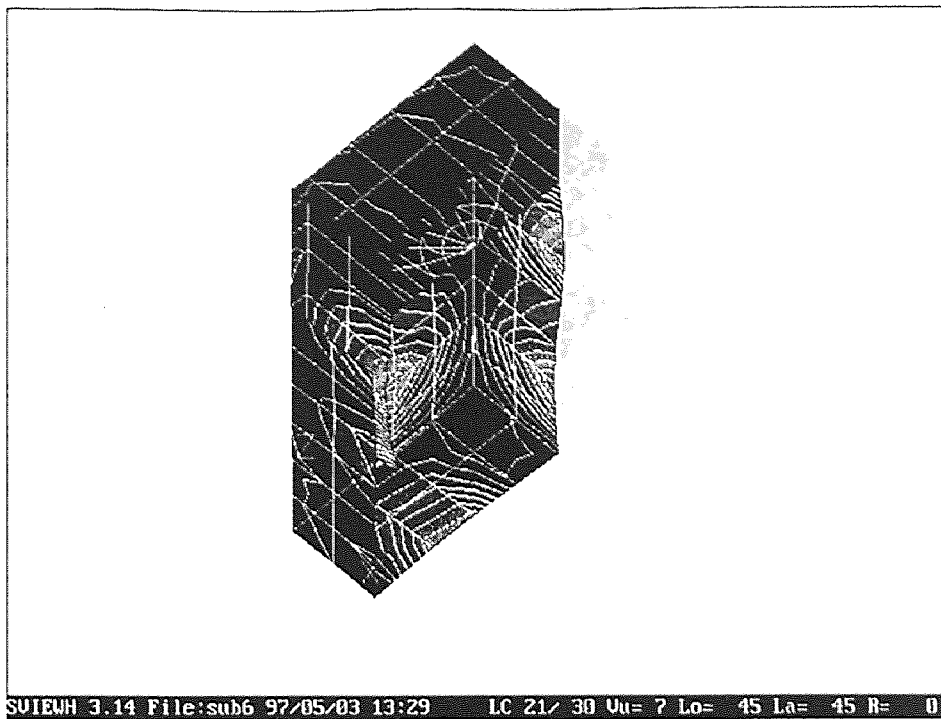


Figure G.21 Enclosure Mode Shape 21:  $f = 1030.0$  Hz

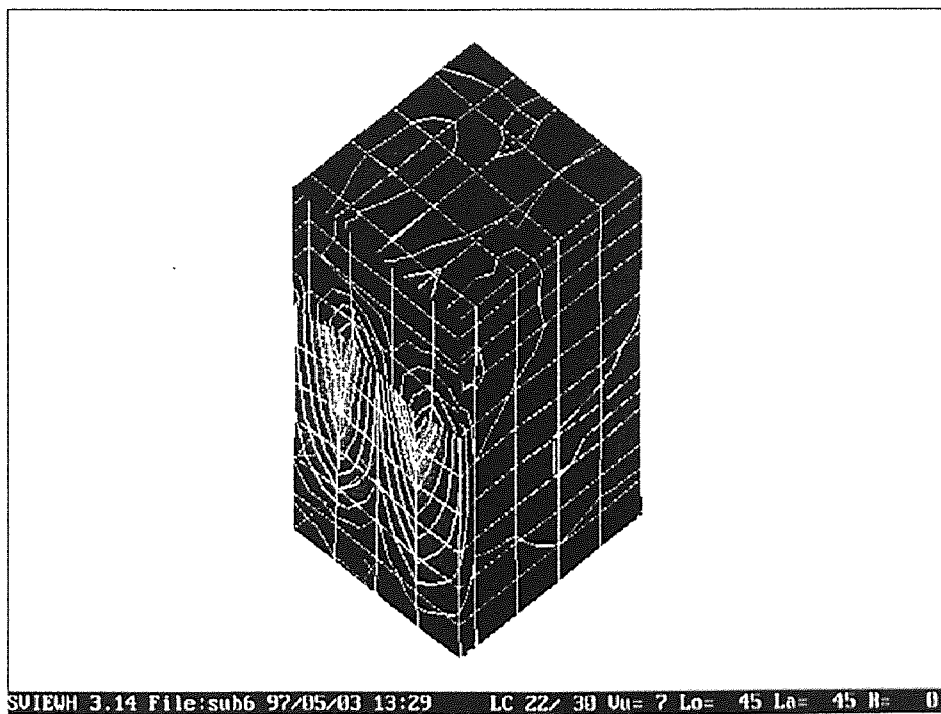


Figure G.22 Enclosure Mode Shape 22:  $f = 1037.9$  Hz

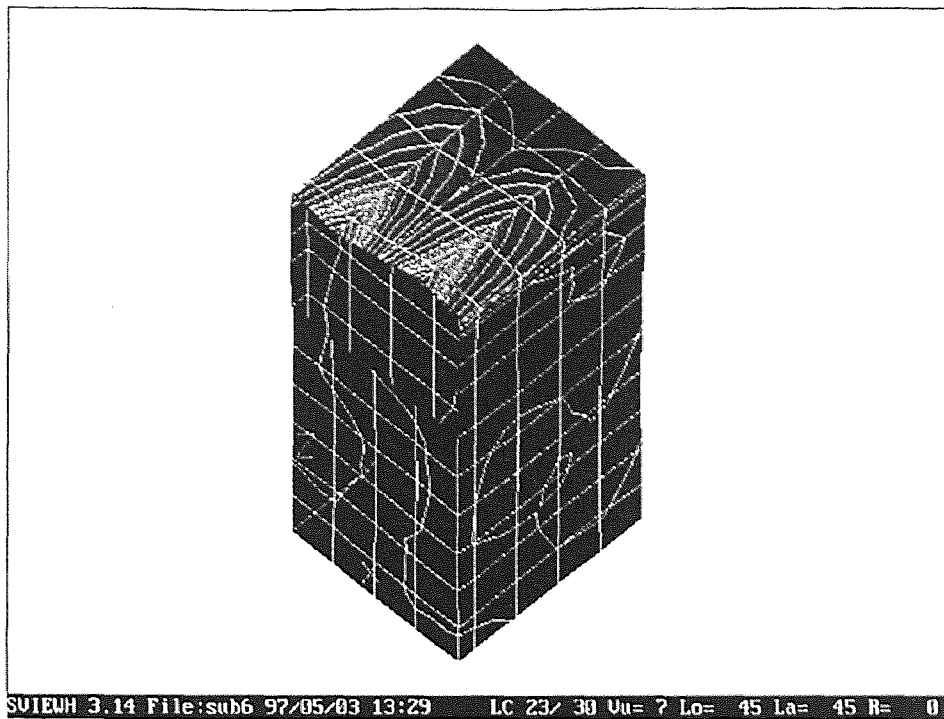


Figure G.23 Enclosure Mode Shape 23:  $f = 1046.4$  Hz

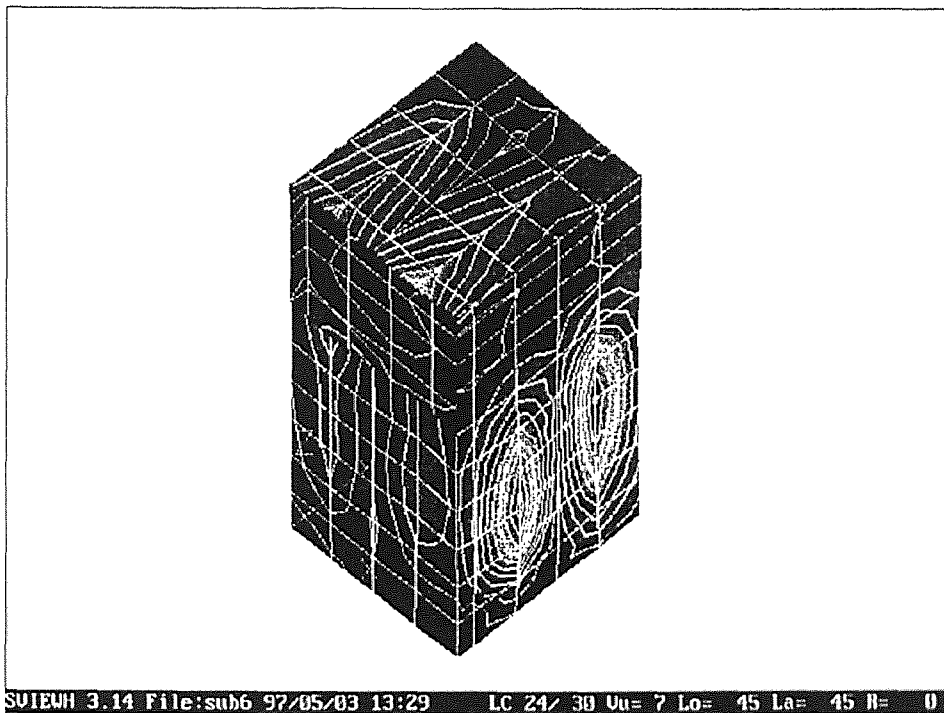


Figure G.24 Enclosure Mode Shape 24:  $f = 1096.4$  Hz

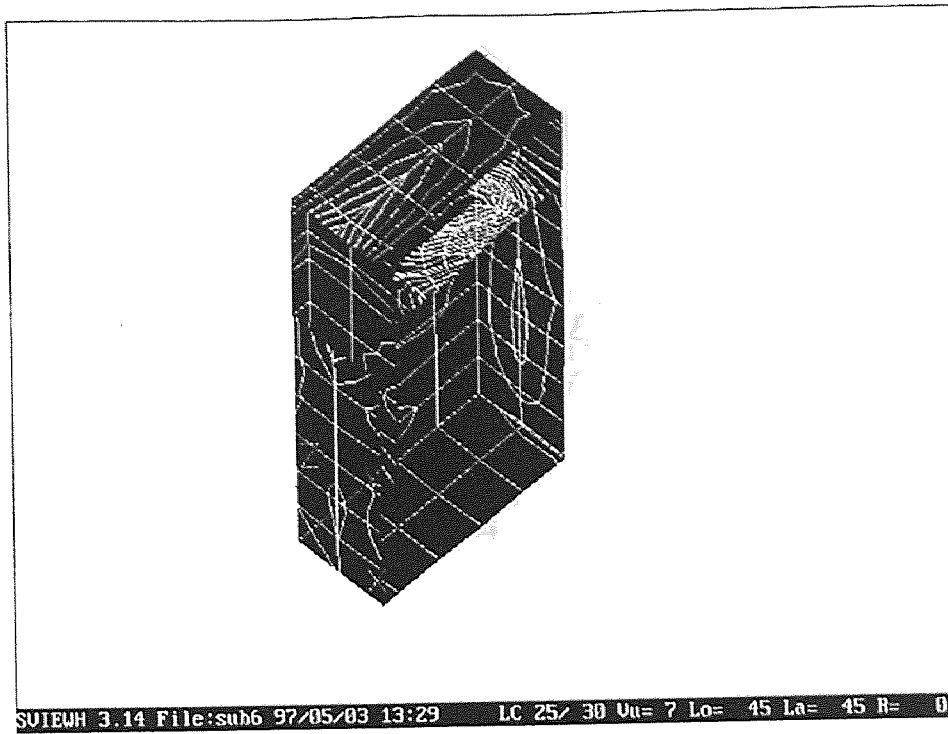


Figure G.25 Enclosure Mode Shape 25:  $f = 1122.2$  Hz

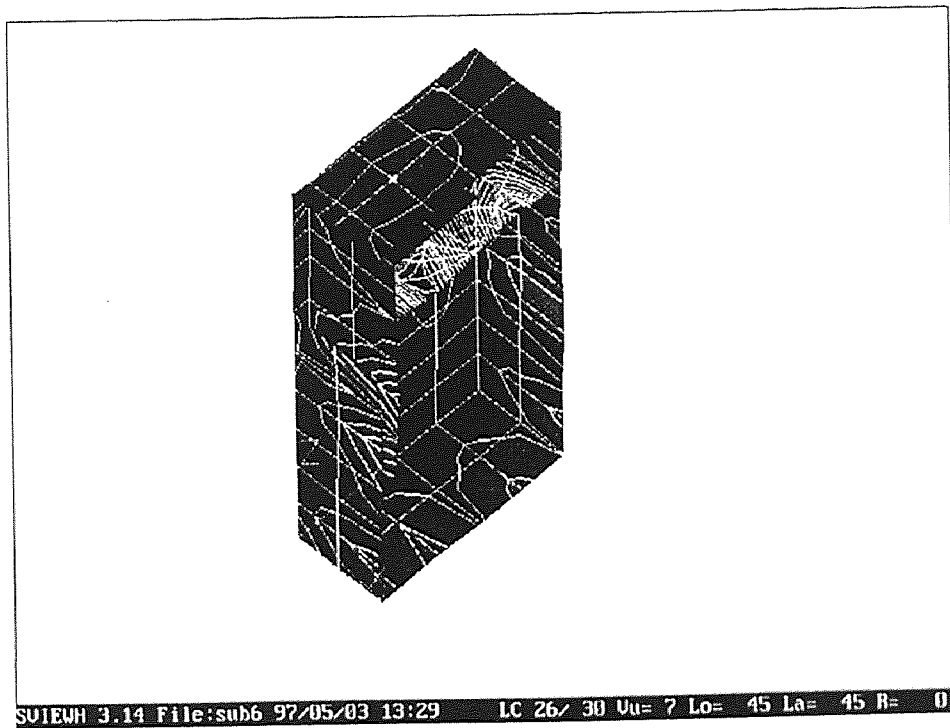


Figure G.26 Enclosure Mode Shape 26:  $f = 1131.5$  Hz



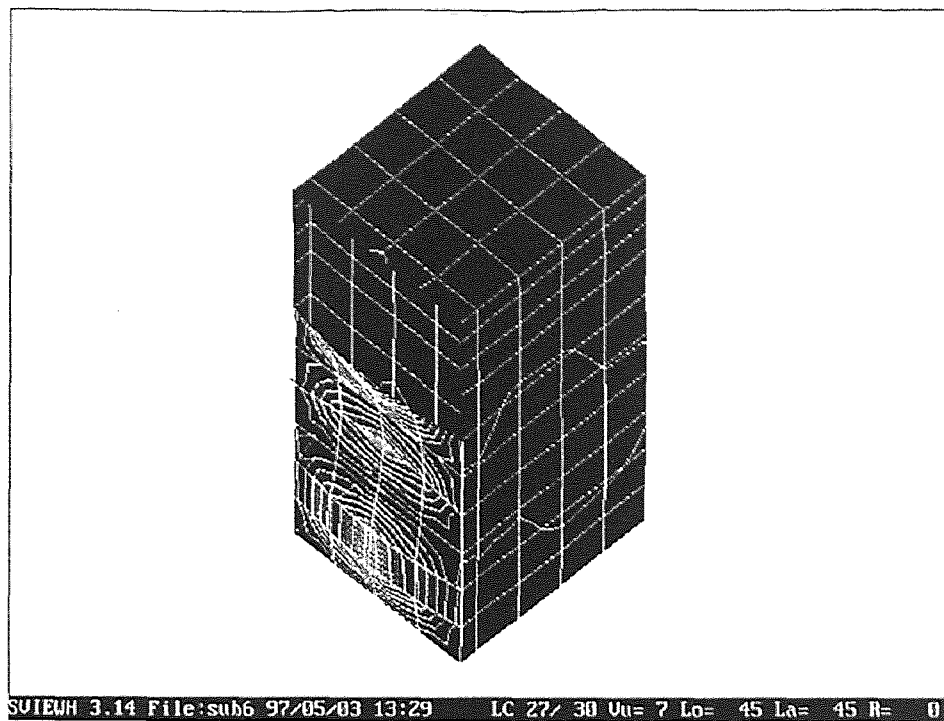


Figure G.27 Enclosure Mode Shape 27:  $f = 1223.4$  Hz

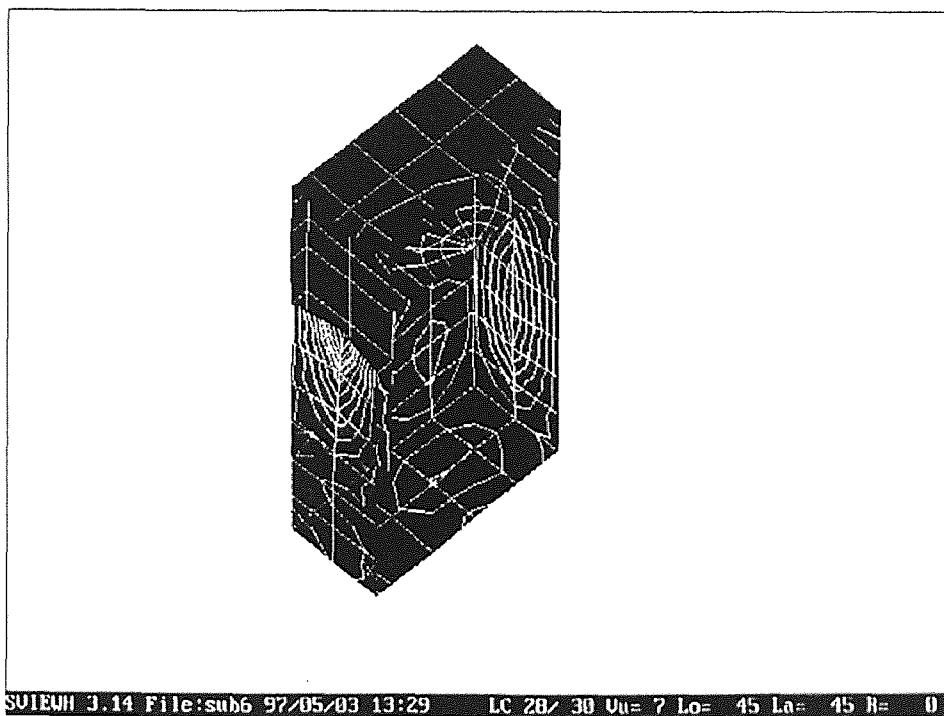


Figure G.28 Enclosure Mode Shape 28:  $f = 1247.6$  Hz

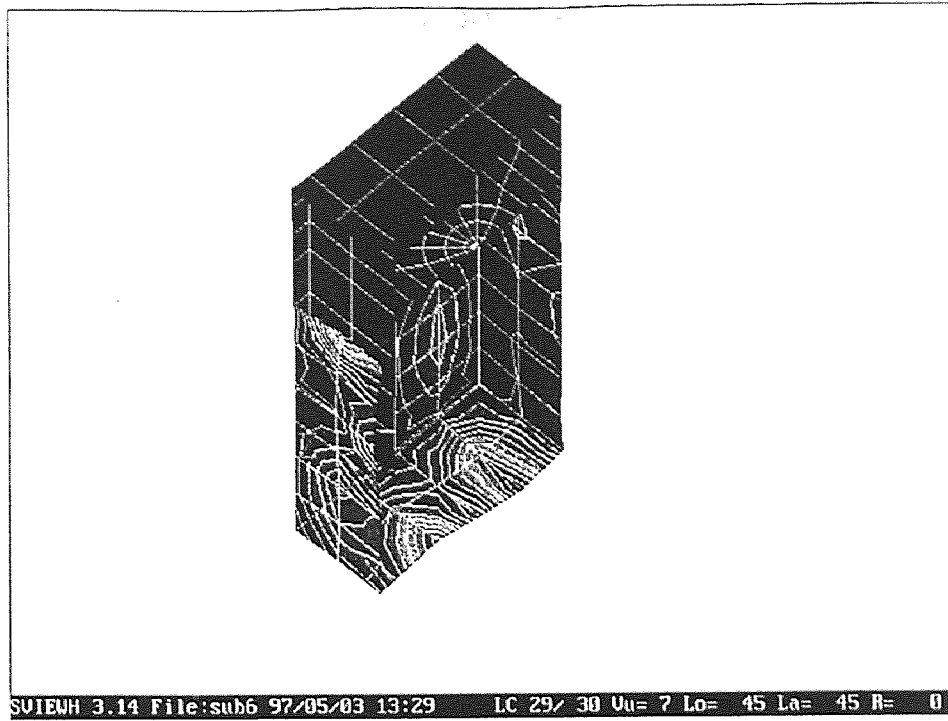


Figure G.29 Enclosure Mode Shape 29:  $f = 1290.2$  Hz

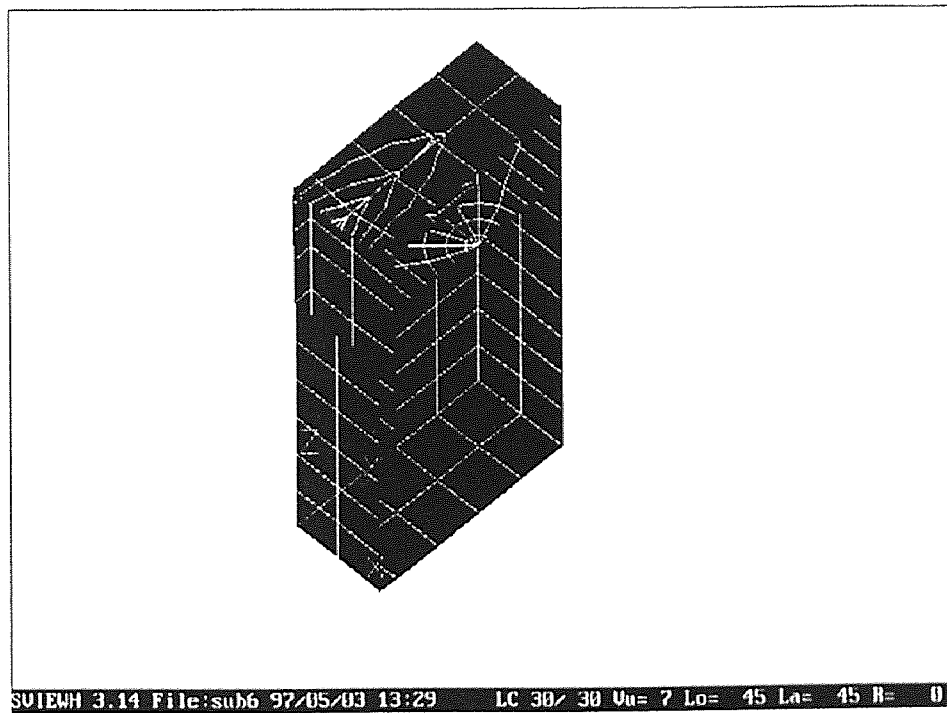


Figure G.30 Enclosure Mode Shape 30:  $f = 1292.1$  Hz

## REFERENCES

1. J. P. Maxfield and H. C. Harrison, "Methods of High Quality Recording and Reproducing of Music and Speech Based on Telephone Research," *Transactions of the American Institute of Electrical Engineers*, vol. 45, pp. 334-348, Feb. 1926.
2. A. E. Kennelly and G. W. Pierce, "The Impedance of Telephone Receivers as Affected by the Motion of Their Diaphragms," *Proc. AAAS*, vol. 48, Sept. 1912.
3. A. E. Kennelly and H. A. Affel, "The Mechanics of Telephone Receiver Diaphragms, as Derived from Their Motional Impedance Circles," *Proc. AAAS*, vol. 51, Nov. 1915.
4. O. Lodge, British Patent No. 9712, 1898.
5. B. B. Bauer, "Equivalent Circuit Analysis of Mechano-Acoustic Structures," *Transactions of the IRE*, vol. AU-2, pp. 112-120, July - August 1954.
6. L. L. Beranek, *Acoustics*, McGraw-Hill, New York, 1954.
7. A. N. Thiele, "Loudspeakers in Vented Boxes," *Proc. of the IREE Australia*, Vol. 22, pp. 487-508, August 1961.
8. R. H. Small, "Direct Radiator Loudspeaker System Analysis," *Journal of the Audio Engineering Society*, Vol. 20, No. 5, 1972.
9. R. H. Small, "Closed-Box Loudspeaker Systems," Part 1: "Analysis," *Journal of the Audio Engineering Society*, Vol. 20, No. 10, 1972; Part 2: "Synthesis," *Journal of the Audio Engineering Society*, Vol. 21, No. 1, 1973.
10. R. H. Small, "Vented-Box Loudspeaker Systems," Part 1: "Small Signal Analysis," *Journal of the Audio Engineering Society*, Vol. 21, No. 5, 1973; Part 2: "Large Signal Analysis," *Journal of the Audio Engineering Society*, Vol. 21, No. 6, 1973; Part 3: "Synthesis," *Journal of the Audio Engineering Society*, Vol. 21, No. 7, 1973; Part 4: "Appendices," *Journal of the Audio Engineering Society*, Vol. 21, No. 8, 1973.
11. W. M. Leach, Jr., "Computer-Aided Electroacoustic Design with SPICE," *Journal of the Audio Engineering Society*, Vol. 39, No. 7/8, July - August 1991.
12. E. R. Geddes, "An Introduction to Band-Pass Loudspeaker Systems," *Journal of the Audio Engineering Society*, Vol. 37, No. 5, May 1989.

13. I. Cochin, H. J. Plass, Jr., *Analysis and Design of Dynamic Systems*, Second Edition, Harper Collins Publishers, New York, 1990.
14. I. H. Shearman, "Assessment of Loudspeaker Quality," *Proc. IREE Australia*, Vol. 31, p.165, June 1970.
15. R. H. Small, "Simplified Loudspeaker Measurements at Low Frequencies", *Proc. IREE Australia*, Vol. 32, pp. 299-304, August 1971.
16. D. B. Keele, Jr., "Low Frequency Loudspeaker Assessment by Nearfield Sound-Pressure Measurement," *Journal of the Audio Engineering Society*, Vol. 22, No. 3, April 1974.